Point-by-point reply to comments of both reviewers for manuscript submitted to HESS, *hess-2018-310*

By Maik Renner and co-authors

November 21, 2018

This document collects all comments and replies to the reviewers into a single document and highlights how the draft was adapted during revision. Detailed replies to the reviewer comments can be found on the discussion page of the manuscript `https://www.hydrol-earth-syst-sci-discuss.net/hess-2018-310/`.

We repeat each reviewer comment in bold font, followed by our reply. Changes in the text of the main manuscript are highlighted in blue color. A track changes version is attached to this reply, with changes highlighted in dark-orange.

Title

We changed the title to be more descriptive of the work and put emphazis into the phase lag analysis.

Old Title: "Understanding model biases in the diurnal cycle of evapotranspiration: a case study in Luxembourg"

New Title: "Using phase lags to evaluate model biases in simulating the diurnal cycle of evapotranspiration: a case study in Luxembourg".

Detailed replies

Reviewer 1: "The study attempts to assess the model biases in the diurnal cycles of evapotranspira- tion and to analyze the influence of observed input variables under dry and wet condi- tions. Much effort has been undertaken to analyze a wealth of observed and modeled data. The approach applied in this study is relatively logical. The findings in the paper may be rational. Therefore, I appreciate the authors' effort to handle such much work. However, I have one concern on the presentation. The paper would be publishable in HESS after minor revisions if the author satisfactorily address my concerns."

Reply: We thank the reviewer for his careful review. We tried to address all concerns and improve clarity.

Reviewer 1: "Lines 22-30 in page 1, This part should be simplified and keep concise for good readability."

Reply: The reviewer refers to the abstract which includes most findings of the study in a very condensed way. To improve the readability we simplified and focussed on our main findings and rewrote the abstract as follows:

Abstract: *While modeling approaches of evapotranspiration (λE) perform reasonably well when evaluated at daily or monthly time scales, they can show systematic deviations at the sub-daily time scale, which results in potential biases in modeled λE to global climate change. Here we decompose the diurnal variation of heat fluxes and meteorological variables into their direct response to incoming solar radiation (Rsd) and a phase shift to Rsd. We analyze data from an Eddy-Covariance station at a temperate grassland site, which experienced a pronounced summer drought. We employ three structurally different modeling approaches of λE, which are used in remote sensing retrievals and quantify how well these models represent the observed diurnal cycle under clear sky conditions. We find that energy balance residual approaches, which use the surface-air temperature gradient as input are able to reproduce the reduction of the phase lag from wet to dry conditions. However, approaches which use the vapor pressure deficit (Da) as driving gradient (Penman-Monteith) show significant deviations from the observed phase lags, which is found to depend on the parameterization of surface conductance to water vapor. This is due to the typically strong phase lag of 2-3h of Da, while the observed phase lag of λE is only in the order of 15 min. In contrast, the temperature gradient shows phase differences in agreement with the sensible heat flux and represents the wet-dry difference rather well. We conclude that phase lags contain important information on the different mechanisms of diurnal heat storage and exchange, and, thus allow a process-based insight to improve the representation of land-atmosphere interactions in models.*

Reviewer 1: "Lines 20-23 in page 2, This study focus on revealing the model biases of evapotranspi- ration by multivariate metrics, therefore recent literatures should be summarized such as Zhou et al., (2018, published in ACP, doi: 10.5194/acp-18-8113-2018) and Zhou et al., (2017, published in JC, doi: 10.1175/JCLI-D-16-0903.1) that investigated the model biases of regional warming in current reanalysis products and attributed those to the modeled land-atmosphere energy budgets and precipitation frequency."

Reply: We thank the reviewer for his suggestions on recent literature. The mentioned papers are well suited as references since these use statistical relationships of different model variables, such as temperature and incoming solar radiation (Zhou et al., 2018, 2017). Differences in these relationships between models and observations highlight different sensitivities and helps to evaluate models in a systematic way. We included these references in the introduction:

Also statistical metrics exploring the strength of linear relationships between surface heat fluxes and states to surface radiation components have been employed to evaluate the performance of reanalysis with observations (Zhou and Wang 2016, Zhou et al., 2017, 2018).

Reviewer 1: "Section Introduction in pages 2-4, some recent relevant literatures should be sum- marized in the paper, such as van Heerwaarden et al., (2010, published in JC, doi: 10.1175/2010JHM1272.1)"

Reply: We thank the reviewer for pointing us to the paper by van Heerwaarden et al. (2010). We updated the introduction and included this valueable reference paper as follows:

These interactions are particularly dominant at the diurnal time scale (e.g. De Bruin and Holtslag 1982) and depend on meteorological as well as on surface conditions (Jarvis and McNaughton, 1986; van Heerwaarden et al., 2010).

Reviewer 1: "Lines 11-21 in page 5, There are other approaches to regress this type of the response. Some reasons of the selection of the Camuffo-Bernardi equation should be provided for good readability."

Reply: We agree with the reviewer that the choice for the Camuffo-Bernardi model should be better motivated, since we have good reasons to use it. We added the following paragraph to the introduction:

Here, we choose the Camuffo and Bernardi (1982) model because it provides an objective measure of the magnitude of hysteresis loops and it allows for an assessment of statistical significance. We extend the Camuffo and Bernardi (1982) model in two ways. First, we use incoming solar radiation (Rsd) as reference variable instead of net radiation to estimate the phase lag of surface heat flux observations and models. And secondly, we use a harmonic transformation of the Camuffo and Bernardi (1982) regression model to estimate the phase lag in time units. This extension allows to compare the diurnal phase lag signatures of the different model inputs and how these influence the resulting diurnal course of the latent heat flux estimate.

Reviewer 1: "Lines 25-end in page 8, The average gap is up to 67 Wm-2 and then the diurnal cycle may has a larger gap. How to quantify the influence of energy balance closure gap (before and after correction) on the magnitude and phase lag in the paper?"

Reply: To assess the potential impact of the closure method we also computed the phase lag statistics for the non-corrected latent heat flux (see Figure 7, Tables 3 and 4). Results show that the phase lag estimates are very similar showing that the correction does not influence magnitude of the observed phase lags.

To improve the communication of this result we adapted P15L11 in the manuscript as follows: *The uncorrected observations showed only a slightly lower wet-dry difference, highlighting that the method to close the energy balance closure gap does not significantly influence the estimated phase lag.*

We also identified a typo in reporting the average energy balance closure gap on P8L31. It is 37 Wm^{-2} instead of 67 Wm^{-2}. We updated the text as follows: *For our site we observed on average a slope of* $(H+\lambda E)\ (Rn\breve{}G) = 0.81$ *(by linear regression) with an average gap of* 37 Wm^{-2} *over the whole duration of the field campaign.*

Reviewer 1: "Line 21 in page 22, how to justify the sentence ('These interactions are also affected by soil water availability, as reflected in the phase lags.') in the paper? whether adding related literatures or not?"

Reply: We replace this sentence with: *We also found that the phase lag of the turbulent heat fluxes is affected by soil water availability.*

Reviewer 1: "Section Conclusions in pages 25-26, The author should rewrite this part to make its logic smooth. If necessary, some discussion should be added to help the readers understand the importance and advantages of this study."

Reply: We agree with the reviewer and revised the first paragraph of the conclusions.

We analyzed the relationship of surface heat fluxes and states to incoming solar radiation at the sub-daily timescale for a temperate grassland site which experienced a summer drought. Most variables showed significant hysteresis loops which we objectively quantified by a linear component and a non-linear phase lag component using *multiple linear regression and harmonic analysis. We then compared these diurnal signatures obtained from observations of an Eddy-Covariance station with commonly used but structurally different approaches to model actual and potential evapotranspiration. The models have been forced by the observational data such that the differences to observations can be attributed to model formulation and signals contained in the input data. Our analysis guides model selection with a preference for the temperature gradient approaches, because the vertical temperature gradient contains relevant signals of soil moisture limitation as opposed to the vapor pressure deficit of the air.*

Replies to reviewer 2

Reviewer 2: "The author's objectives of the study were to use measurements of hourly incoming shortwave radiation as an independent forcing of the land-atmosphere exchange and assess the response and phase lags of surface heat fluxes. The authors argue that models of ET should be able to capture the magnitude of hysteretic loops under differ- ent conditions."

Reply: We agree with this summary of the manuscript.

Reviewer 2: "The writing is good, and the article is well structured. The major concern I have is that incoming solar radiation (Rsd) is used rather than the available energy (Rn-G)."

Reply: Our main reasoning is that available energy is not an independent variable as it depends on surface temperature. We added a paragraph in the introduction to explain our reasoning:

We specifically choose incoming solar radiation Rsd as the reference for the phase shift analysis, since Rsd can be regarded as an independent forcing of the surface energy balance (e.g. Ohmura (2014)):

$$R_{sd}(1-\alpha) + R_{ld} - H - \lambda E - G = \sigma T^4 + m \tag{1}$$

With surface albedo α*, incoming longwave radiation Rld, sensible heat flux H, latent heat flux* λE*, the conductive soil heat flux G, the outgoing longwave radiation* σT^4 *and storage terms of the surface layer summarized in m. This form of the surface energy balance provides the direction of the energy exchange processes at the surface, illustrating that the terms on the right-hand side depend on heat fluxes on the left-hand side of Eq. (1) (Ohmura 2014). As a consequence, the term net radiation Rn, which resembles the radiation budget of the shortwave and longwave components:* $R_n = R_{sd}(1-\alpha) + R_{ld} - \sigma T^4$*, cannot be regarded as an independent surface forcing. Therefore, we prefer to use Rsd instead of Rn or Rn-G as the reference variable for phase shift analysis of the latent heat flux and the main input variables of evapotranspiration model approaches.*

Reviewer 2: "“It is expected that phase lags would occur between R_{sd} and LE since much energy is stored in the ground surface during the day and then released at night, so it is unclear what the novel aspects of the paper really are.” “By not considering G, you get phase lags. . . is there something novel to see here?”"

Reply: The reviewer is unclear about the novelty of our findings and states that we find a phase lag (e.g. to the Latent heat flux but also to Potential evapotranspiration”) because we use Incoming Solar Radiation and not Available Energy ($R_n - G$) as reference variable. The argument being that the phase lag we observe is mainly caused due to heat storage in the soil as reflected by the soil heat flux.

We disagree on this perspective. First of all the soil heat flux is not sufficient to buffer the diurnal imbalance caused by solar heat of the land surface. Most of the diurnal imbalance is buffered in the lower atmosphere leading to the development of a convective boundary layer (Oke, 1987). To substantiate our argument we repeated to phase lag analysis with Available Energy ($R_n - G$) as reference variable. We added the resulting phase lag as another column to Table 4 of the manuscript. Overall, there is only a minor difference of the phase lag between the two reference variables. This is to be expected since R_{sd} has the largest diurnal variations of the components of Available Energy. There is only a minor reduction of phase lag (3 min) with respect to the evapotranspiration estimates. This highlights that the soil heat flux is not the main cause of the observed phase lag of the turbulent heat fluxes.

Reviewer 2: "Page 3 Line 16: Why is Rn not used? Better yet, why isn't Rn-G (available energy) used? I don't see that why Rn (and Rn-G) is not used if the authors are indeed trying to better understand controls on LE. . . longwave radiation is a big component of Rn, and G lags no doubt control some of this hysteresis. I feel that the authors are missing too much energy if they just focus on Rsd.
Page 3 Line 23: The PT equation requires Rn, not Rsd, so how can you say you focus on using Rsd, but use the PT equation and not use Rn? Same with the PM equation. Please explain how and if Rs is used in these equations here and you can go into greater detail in the methods if needed. "

Reply: Our analysis focusses on the diurnal relation of evapotranspiration and relevant surface energy balance fluxes and states to incoming solar radiation. Since Rsd is independent of the surface, it is an ideal reference to calculate phase lags. We acknowledge that all models which we compare in this study actually use available energy (net radiation - ground heat flux) (Rn-G) as an input variable, which would also justify to directly use Rn as a reference for the phase lag analysis which is suggested by the reviewer. The differences in the obtained phase lag using Rsd or Rn are not substantial, see updated Table 4.

We added a paragraph to the results section 3.3: *Since all evapotranspiration schemes use Rn-G as forcing, we also computed that phase lags with Rn-G as reference variable (see Table 4). The difference to Rsd as reference are, however, rather small with slightly lower phase lags and in the range of the standard deviation of the daily estimates. This is because there is hardly any phase lag between Rsd and Rn and because the magnitude and the phase lag of the soil heat flux is rather small.*

We also think that this result needs to be better discussed and added a paragraph to the first section of the discussion: *It is important to emphasize here, that the phase lags we found here are not dominated by diurnal heat storage changes below the surface. The phase lag of the soil heat flux to Rsd is smaller than the phase shifts of the turbulent heat fluxes. All models we employ here use available energy (Rn − G) as input to estimate LE. So one may think that the identified phase lags are due to choosing Rsd as the reference. However, the phase lag of the latent heat flux would only reduce by about 3 min when one would choose Rn-G instead of Rsd as reference variable to calculate the phase lags. This is because there is almost no phase lag between Rn and Rsd and the fact that both the magnitude and the phase lag of the soil heat flux are relatively small.*

Reviewer 2: "Additionally, descriptions of what was assumed or used as input to the models, (specifically the PT and FAO-56 PM equations) is not adequate, only Rn is in the PT equation listed, not Rn-G as stated in the original equation, so there could be an error in the analysis. It is unclear if measured G was used in the FAO-56 PM equation, or if it was estimated, and same goes for Rn. Based on the lack of clarity as to what Rn and G model was used in the FAO-56 approach, those results cannot be assessed as is. While there is some good discussion on process, the novelty of the study is lacking."

Reply: We believe that there are some misunderstandings, which we tried to resolve in our first reply to Reviewer 2, please see (`https://doi.org/10.5194/hess-2018-310-AC1`). All models have been driven by the observational data which is important because this allows a fair comparison between models. A list of input is provided in Table 2 of the manuscript.

Specifically, both potential evapotranspiration estimates, the Priestley-Taylor evapotranspiration and FAO Penman-Monteith estimate, use available energy ($R_n - G$) as input. We apologize that the soil heat flux was missing in the Priestley-Taylor Equation (Eq. 7) and corrected this typo in the revision. The calculations are, however, not affected by this typo. Also, the FAO Penman-Monteith equation was driven with net radiation and soil heat flux from the observations and not from one of the empirical replacements as provided in the FAO-56. Hence we can assure that the findings of systematically different diurnal cycles of the Penman-Monteith driven models is indeed related to the model formulation and not to errors in the analysis.

All code (and data) to reproduce the analysis are provided in a public accessible repository with this revision of the manuscript.

Reviewer 2: "Perhaps a more useful and/or complementary analysis would be to focus on the hourly distribution of the energy balance closure ratio, and assess the controlling factors of the distribution, if any, as it relates to soil moisture and other conditions."

Reply: While the analysis of the energy balance closure was not a focus of our work, we actually considered potential impacts by the way the energy balance was closed (instantaneous closures using a daily mean Bowen Ratio). To assess the potential impact of the closure method we also computed the phase lag statistics for the non-corrected latent heat flux (see Figure 7, Tables 3 and 4). Results show that the phase lag estimates are very similar showing that the correction does not influence magnitude of the observed phase lags.

To improve the communication of this result we adapted P15L11 in the manuscript as follows: *The uncorrected observations showed only a slightly lower wet-dry difference, highlighting that the method to close the energy balance closure gap does not significantly influence the estimated phase lag.*

Reviewer 2: "Pg 2 Line 29-30: LE is strongly correlated with Rsd, not the other way."

Reply: The text was adapted.

Reviewer 2: "Pg 2 Line 21-22: Would be good to give a quick summary of these metrics, and why some are more useful than others if they are to be used or referenced later. This would be good so that when the alternative metric is proposed below the reader has some context."

Reply: We agree with the reviewer that the introduction needs a better motivation on the existing metrics.

Therefore we provide a summary of the different metrics in use and explain why we are using the metric of a phase lag.

There is a strong need to investigate and to derive metrics based on comprehensive observation that characterize the whole land surface-atmosphere system (Wulfmeyer et al. 2018). Several authors proposed different multivariate metrics to better evaluate land-atmosphere (L-A) interactions in observations and models. Generally, these metrics explore internal relationships between state variables to better characterize key processes and to guide a more systematic exploration and understanding of model deficiencies. A number of ***metrics*** *focus on the diurnal evolution of the* ***heat and moisture budgets in the planetary boundary layer*** *(e.g., Betts 1992, Santanello et al. 2009, Santanello et al., 2017). Also* ***statistical metrics*** *exploring the strength of linear relationships between surface heat fluxes and states to surface radiation components have been employed to evaluate the performance of reanalysis with observations (Zhou and Wang 2016, Zhou et al., 2017, 2018). Furthermore, there are* ***pattern-based metrics*** *which focus on non-linear interactions at the diurnal time scale. Wilson et al., (2003) proposed the method of a diurnal centroid to measure the timing of the surface heat fluxes and their timing difference, which was more recently used by Nelson et al., 2018 to quantify the timing of evapotranspiration under different dryness condition for the FLUXNET dataset. In contrast Matheny et al., 2014 and Zhang et al., 2014 explored the diurnal relationship of the latent heat flux to vapor pressure deficit showing a pronounced hysteresis loop. Zheng et al., 2014 also included air temperature and net radiation as references variables and showed that the hysteresis loops of* λE *to* D_a *or* T_a *are large, while there are only small hysteresis effects when Rn was used. Hysteresis loops have also been found when heat fluxes plotted against net radiation (Camuffo and Bernadi 1982; Mallick et al., 2015), with many studies showing hysteretic loops of the soil heat flux against net radiation (Fuchs and Hadas, 1972; Santanello and Friedl, 2003; Sun et al., 2013). The presence of an hysteresis loop indicates that there is a time dependent non-linear control on the variable of interest, typically induced by heat storage processes. Camuffo and Bernardi (1982) showed that the magnitude and direction of such hysteretic loops can be estimated by a multi-linear regression of the variable of interest against the forcing variables and its first order time-derivative. This simple model allows to estimate storage effects on diurnal (Sun et al. 2013) to seasonal time scales (Duan and Bastiaansen 2017).*

Reviewer 2: "Pg 3 Line 2: I don't think that the other controls (other than Rn and Rsd) on LE remains unclear. . . it is pretty simple from an energy balance perspective (which is what is being discussed so far in terms of Rn and Rs) . . . LE = Rn – H – G . . . Lots to dig into with H obviously. . . and G, and perhaps that is where some of the controls need more study?"

Reply: We believe that writing the energy balance with $R_n = \lambda E + H + G$ is sufficient when direct measurements are used. However, when modeling the problem it is clear that all terms may depend on each other. For a mechanistic understanding a full treatment of the surface energy balance with explicit treatment of all radiation components is required. Reviewer 1 pointed to a recent study by van Heerwaarden et al. (2010) which discusses the complex interactions of at the surface, the surface layer and the planetary boundary layer, all feeding back on LE. The importance of controls on LE must be considered unclear, since there exist different schemes with different input variables to model LE. Many of the input variable are themselves strongly affected by the land-atmosphere exchange and its feedbacks.

Reviewer 2: "Page 4 Line 7: but RH and VPD is coming from gridded weather data, no? So this is a forcing and outside the evaporation model, correct?"

Reply: The reviewer mentioned the MOD16 algorithm which was compared with other approaches with surface observations in Yang et al. (2015). That approach uses VPD as an input variable (forcing) which depends on air temperature. While there is some uncertainty when RH and VPD is obtained from coarse reanalysis products instead of in-situ observations, the main physical argument is that VPD (temperature) of the air cannot resolve the spatial variability of surface water limitation as compared to surface temperature.

Reviewer 2: "Page 6 Line 28-34: This is concerning since the heat storage in the soil slab above the G plate was estimated rather than measured. Sounds like the estimate didn't con- sider changes in soil moisture, which is a big factor in the potential to store heat within soils. Any errors in the estimate, or bad heat storage measurements could cause "perceived hysteresis" when comparing to other energy balance components. When was the harmonic calibrated, to dry or wet conditions, or both? Did the harmonic behave differently (have different parameters) when assessed during wet vs dry conditions as anticipated?"

Reply: The total ground heat flux can be obtained by measuring the soil heat flux at a given depth and an correction based on an estimate of heat storage changes above the heat flux plate (Massman 1992). The preferred method for the heat storage changes above the heat flux plate are soil temperature measurements. However, the upper soil temperature sensor failed after two weeks and the following period was characterized by a longer dry period. To circumvent this problem we used an alternative method based on a harmonic transformation of the heat flux plate measurements. The critique of the reviewer is that we did not take the soil moisture dependency of this method into account. This method requires an estimate of the damping depth D which was obtained by the exponential decay of the temperature amplitude of soil temperature measurements.

D is proportional to the square root of the thermal diffusivity and is only weakly dependent on soil moisture for clayey soils above 0.1 m3 m-3 water content (Jury and Horton, 2004) we had at our site. For the present work, D was determined by the exponential decay with depth of the soil temperature amplitude measured for the diurnal cycle in 2, 5, 15, and 30 cm depth at 15 different days between 12th June and 4th July. The mean of 12.27 ± 0.91 cm of these determinations was used for harmonic analysis. As mentioned in the manuscript, the upper soil sensors began to fail after 30th June and no determinations of D were possible after 4th July. Ten (five) determinations were performed for soil moisture contents >15% (<15%) where D was obtained to 12.55 ± 0.65 cm (11.71 ± 1.15 cm). The differences between the calculated ground heat fluxes using $D = 12.27cm$ and $D = 12.55$ and $D = 11.71cm$, respectively, were always $< 10Wm^{-2}$ so that the used value of $D = 12.27cm$ is a good compromise. For the data until 30th June we find a linear relationship with a slope of 1.05 and $R^2 = 0.94$ for the ground heat flux calculated with harmonic analysis of the HFP fluxes and the heat flux plate method with correction for heat storage. Please also find a figure attached to this reply which shows the diurnal cycles of the total soil heat flux estimates obtained by the upper soil temperature measurements (magenta) and the soil heat flux from the harmonic correction of the soil heat flux plate (blue). The plot only shows sunny days used in the analysis and also reports the top soil moisture of that day. The plots shows higher soil heat fluxes under the wetter conditions for both methods. We thus consider that the total soil heat flux obtained by the harmonic correction of the soil heat flux plate characterizes the diurnal dynamics of the soil heat conduction rather well.

We will added a summary of this explanation to the description in section 2.2: *Unfortunately, the two upper temperature probes and soil matric potential sensors showed data gaps and erroneous values from 30 June until excavation on 23 July, 2015. Thus, the ground heat flux was calculated by the heat flux plate method with correction for heat storage (Massman, 1992) only for the period from 11 June to 30 June, 2015. To still obtain soil heat fluxes for the entire measuring period, additionally harmonic wave analysis (Duchon and Hale, 2012) of the heat flux plate data was applied. The harmonic wave analysis calculates the wave spectrum at the soil surface from the Fourier transform of the soil heat flux measured by the heat flux plates in a few cm depth (here: 8 cm) by correcting for wave amplitude damping and phase shift. The surface ground heat flux is then obtained by an inverse Fourier transformation of the corrected wave spectrum. The method has a dependence on soil moisture affecting the damping depth. The dependence is, however, weak for clayey soils with soil water contents > 10% (Jury and Horton 2004) as observed at the site. The damping depth was obtained by the exponential decay of the soil temperature amplitude measured at the various depths. Differences in the damping depth between wet and drier soil moisture conditions only yielded differences in G smaller than 10 W m-2. Therefore, we used a constant damping depth for the whole period.*

Reviewer 2: "Page 8 Line 31: What time step was Qgap (the energy balance closure) assessed? Every 30min?"

Reply: Yes, the gap has been determined for each time step.

To correct the turbulent fluxes for the energy balance closure gap (evaluated at the 30 min time steps), we use a correction based on the Bowen ratio (BR) (Twine et al., 2000), which is directly related to the evaporative fraction fE = 1/(BR+1) to obtain corrected fluxes

Reviewer 2: "Page 10 Line 25: The PT equations uses Rn-G, not simply Rn as writ- ten. What did you use? Rn or Rn-G (see equation 14 of the PT paper - ftp://ftp.library.noaa.gov/docs.lib/htdocs/rescue/mwr/100/mwr-100-02-0081.pdf). The phase lag results can't be interpreted until this is cleared up."

Reply: We corrected equation 7 to use (Rn-G). This was also used in the analysis, so the interpretation will not change.

Reviewer 2: "Page 11 Line 14-16: Is Rsd used and then Rn and G is estimated following the procedures of FAO-56, or is the measured Rn-G used? This needs to be spelled out to understand the results."

Reply: Our strategy is to use all model forcing directly from the observations. The procedures of FAO are only recommended when input data is missing. We added one sentence to make this clear: *. Here we use the latter definitions of the conductances and use direct measurements for the other input variables to equation (9) to obtain the FAO Penman-Monteith estimate.*

Reviewer 2: "Figure 6. Be consistent calling incoming shortwave Rsd vs Global radiation. . . you say both."

Reply: Thank you for pointing this out. We updated the figures labels of Figures 6, 8, 9 and 11 accordingly.

Reviewer 2: "Figure 7 isn't very useful since it is Rsd on the x, and not Rn-G. I guess I don't see the point since phase lag is to be expected (and greater for wet conditions as shown), and it is unclear how G was considered in the FAO approach."

Reply: This comment regards the question of using Rsd or Rn as reference to quantify the phase lag. We already replied to this in a separate author reply. With respect to Figure 7, which shows the phase lag of the different latent heat flux estimates against Rsd we find a general wet-dry difference in the observations and most models but not for the Penman-Monteith based approaches. We also computed the phase lag of the key model input parameters in Fig 12. The reviewer suggested to used Rn-G as a reference. Doing this will not change Figure 7 much and thus also not the conclusions. See also the updated Table 4.

Reviewer 2: "Page 17 line 4-5: The authors state that "Generally, there was only a small hysteresis in the available energy (Rn – G) (Table 4)" which is exactly what one would expect if Rn-G was used. So by not including longwave and G there is phase lag, which is to be expected, so I don't see the point of the paper really. . . Also, there would be more phase lag in wet soil conditions, than in dry conditions since heat storage is greater when there is more water in the soil. By not considering G, you get phase lags. . . is there something novel to see here?"

Reply: We already replied to this point. The soil heat flux shows a small phase lag to Rsd which increases in magnitude when wet. However, the phase differences of the turbulent heat fluxes are even larger in magnitude than the ones of G, see Table 4 and Fig.12. These phase lags are also present when Rn-G is used as reference (instead of Rsd). This is consistent with the argument that the soil heat flux is too small to compensate the diurnal imbalance caused by solar radiation. Hence the land-atmosphere heat exchange strongly contributes to balance the large diurnal forcing of solar radiation.

Reviewer 2: "Page 20 and Figure 11: The results of the hysteresis in humidity variables are what you would expect. The VPD is lowest in the morning, and highest in the mid to late afternoon, and largely a function of es, since it is a fairly humid environment, so what is novel here?"

Reply: We believe that the diurnal course of VPD is known to most researchers. The key point is that VPD is used as the driving gradient in the Penman-Monteith approaches. This gradient shows a strong hysteresis loop, while the surface to air temperature difference, which is the driving gradient of the energy balance residual approaches shows only a small hysteresis. Visualizing this difference in the two driving gradients (cf. Fig. 9 and Fig 11) should highlight the key differences in these approaches.

Reviewer 2: "Page 25 Line 22: Yes this was quantified, but it was expected, and it changes in time and space, based on the land surface conditions, and met. forcings."

Reply: We updated the conclusions of the manuscript to improve the clarity of our writing, see also our reply to reviewer 1 above and `https://doi.org/10.5194/hess-2018-310-AC2`.

Reviewer 2: "Page 25 Line 23: Explain exactly how these results have practical application for re- mote sensing based models? This was never fully described, that is why this phase lag issue is so important for remote sensing studies of LE to consider or include."

Reply: The key contribution of the phase lag analysis is that it guides model selection for observational driven LE retrievals, such as remote sensing based approaches. This includes the common measurements for the input of these approaches. As we clearly show they have different phase lags (Fig. 12) and thus influence the resulting LE estimates. We discuss these issues in depth and refer to it in the conclusions. Please note the revised conclusions section, discussed above.

Reviewer 2: "Page 25 Line 30-33: There is too little information on the specifics in the paper of FAO-PM approach applied to assess if this is a correct conclusion."

Reply: As already comment above, we added information on input variables in the text (in addition to Table 2 summarizing the input data).

Other changes

During revision we updated the coefficients of the empirical Magnus equation to calculate the saturation vapor pressure curve and its temperature derivative, see section 2.2.1. We now use more recent coefficients published by Alduchov and Eskridge (1996). This effects the vapor pressure and saturation vapor pressure estimates and thus the Priestley-Taylor and the Penman-Monteith potential evapotranspiration estimates. The changes are, however, very minor (e.g. change in mean LE PM-FAO in Table 3, approx. $1Wm^{-2}$). Tables 3 and 4 and Figures 4-12 have been updated.

References

Alduchov, O. A. and Eskridge, R. E.: Improved Magnus Form Approximation of Saturation Vapor Pressure, Journal of Applied Meteorology, 35, 601–609, doi:10.1175/1520-0450(1996)035<0601:IMFAOS>2.0.CO;2, 1996.

Jury, W. A. and Horton, R.: Soil Physics, John Wiley & Sons, Inc, 6th edn., 2004.

Ohmura, A.: The development and the present status of energy balance climatology, Journal of the Meteorological Society of Japan. Ser. II, 92, 245–285, 2014.

Oke, T.: Boundary layer climates, Routledge, Londan and New York, 1987.

van Heerwaarden, C. C., Vilà-Guerau de Arellano, J., Gounou, A., Guichard, F., and Couvreux, F.: Understanding the Daily Cycle of Evapotranspiration: A Method to Quantify the Influence of Forcings and Feedbacks, Journal of Hydrometeorology, 11, 1405–1422, doi:10.1175/2010JHM1272.1, 2010.

Yang, Y., Long, D., Guan, H., Liang, W., Simmons, C., and Batelaan, O.: Comparison of three dual-source remote sensing evapotranspiration models during the MUSOEXE-12 campaign: Revisit of model physics, Water Resources Research, 51, 3145–3165, doi:10.1002/2014WR015619, 2015.

Zhou, C., Wang, K., and Ma, Q.: Evaluation of Eight Current Reanalyses in Simulating Land Surface Temperature from 1979 to 2003 in China, Journal of Climate, 30, 7379–7398, doi:10.1175/JCLI-D-16-0903.1, 2017.

Zhou, C., He, Y., and Wang, K.: On the suitability of current atmospheric reanalyses for regional warming studies over China, Atmospheric Chemistry and Physics, 18, 8113–8136, doi:https://doi.org/10.5194/acp-18-8113-2018, 2018.

Using phase lags to evaluate model biases in simulating the diurnal cycle of evapotranspiration: a case study in Luxembourg

Deleted: Understanding

Maik Renner[1], Claire Brenner[2], Kaniska Mallick[3], Hans-Dieter Wizemann[4], Luigi Conte[1], Ivonne Trebs[3], Jianhui Wei[4], Volker Wulfmeyer[4], Karsten Schulz[2], Axel Kleidon[1]

[1]Max-Planck Institute for Biogeochemistry, Jena, 07745, Germany
[2]Institut für Wasserwirtschaft, Hydrologie und konstruktiven Wasserbau, Universität für Bodenkultur (BOKU), Wien, 1190, Austria
[3]Department Environmental Research and Innovation, Luxembourg Institute of Science and Technology (LIST), Belvaux, L-4422, Grand-duchy of Luxembourg
[4]Institut für Physik und Meteorologie, Universität Hohenheim, 70599 Stuttgart, Germany

Correspondence to: Maik Renner (mrenner@bgc-jena.mpg.de)

Abstract. While modeling approaches of evapotranspiration (λE) perform reasonably well when evaluated at daily or monthly time scales, they can show systematic deviations at the sub-daily time scale, which results in potential biases in modeled λE to global climate change. Here we decompose the diurnal variation of heat fluxes and meteorological variables into their direct response to incoming solar radiation (R_{sd}) and a phase shift to R_{sd}. We analyze data from an Eddy-Covariance station at a temperate grassland site, which experienced a pronounced summer drought. We employ three structurally different modeling approaches of λE, which are used in remote sensing retrievals and quantify how well these models represent the observed diurnal cycle under clear sky conditions. We find that energy balance residual approaches, which use the surface-air temperature gradient as input are able to reproduce the reduction of the phase lag from wet to dry conditions. However, approaches which use the vapor pressure deficit (D_a) as driving gradient (Penman-Monteith) show significant deviations from the observed phase lags, which is found to depend on the parameterization of surface conductance to water vapor. This is due to the typically strong phase lag of 2-3h of D_a, while the observed phase lag of λE is only in the order of 15 min. In contrast, the temperature gradient shows phase differences in agreement with the sensible heat flux and represents the wet-dry difference rather well. We conclude that phase lags contain important information on the different mechanisms of diurnal heat storage and exchange, and, thus allow a process-based insight to improve the representation of land-atmosphere interactions in models.

Deleted: The diurnal forcing of solar radiation is the largest signal within the Earth system and dominates the diurnal cycle of the turbulent heat fluxes and evapotranspiration (λE) over land. Incoming solar radiation (R_{sd}) also shapes temperature, vapor pressure deficit and wind speed known as important controls on λE. Current process-based λE schemes used in remote sensing and land-surface modeling differ in how these controls on λE are represented and which input variables are required. Here, we analyze how well different surface energy balance schemes are able to reproduce the diurnal cycle and how the diurnal signals of observed input variables actually influence the resulting diurnal pattern of λE. As additional constraint for model evaluation we estimate a linear and a non-linear phase shift component of a surface variable (e.g. λE) to incoming solar radiation. We illustrate our analysis with observations from an eddy covariance station at a temperate grassland site in Luxembourg with a focus on clear sky conditions. During the field campaign in 2015 a summer drought led to a dry-down of soil moisture which allows for studying the effect of wet and dry conditions on the diurnal cycle.

Deleted: We found a remarkable, almost linear relationship of λE with R_{sd}, which exhibits a significant positive phase lag during wet periods. This phase lag in λE was compensated by a preceding phase lag of the sensible heat flux. Vapor pressure deficit (D_a, often used as input for Penman-Monteith based approaches) exhibits a strong phase lag, which is driven by air temperature reflecting large diurnal heat storage changes in the lower atmosphere. This large phase lag in D_a, which is not seen in λE, explains why actual and potential evapotranspiration approaches can show systematic deviations from observations at the sub-daily time scale and highlight the need for a time-dependent non-linear compensation through the conductance parameterization. The surface to air temperature gradient used as input in energy balance residual approaches corresponds rather well with its linear response and phase lag to the observed sensible heat flux under both, wet and dry conditions. This simplifies the conductance parameterization and explains the better correlation of these models at the sub-daily time scale.¶
We conclude that the analysis of phase lags at the sub-daily time-scale provides valuable information on the drivers of the surface-atmosphere exchange, which can be used to evaluate and improve the representation of land-atmosphere coupling in land-surface schemes.¶

1 Introduction

Evapotranspiration and the corresponding latent heat flux (λE) couple the surface water and energy budgets and are of high relevance for water resources assessment. λE is generally limited by four physical factors, (i) the availability of energy mostly supplied by solar radiation, (ii) the availability of and the access to water, (iii) the plant physiology, and (iv) the atmospheric transport of moisture away from the surface (Brutsaert 1982). These different limitations have led to different approaches on how to model λE.

Key approaches either focus on the surface energy balance where the surface-air temperature gradient dominates the flux; or approaches which focus on the moisture transfer limitation where vapor pressure gradients dominate the flux. It is critical to recognize that these two limitations are not independent of each other but rather are shaped by land-atmosphere heat and water exchange and thus covary with each other. The diurnal variation of incoming solar radiation (R_{sd}) causes a strong diurnal imbalance in surface heating leading to the pronounced diurnal cycles of surface states and fluxes (Oke 1987, Kleidon and Renner, 2017). This heat exchange of the surface with the lower atmosphere thus influences the near-surface air temperature (T_a), skin temperature (T_s), vapor pressure (e_a), soil or canopy saturation water pressure (e_s), vapor pressure deficit (D_a), and wind speed (u), that are being regarded as important controls on λE (e.g. Penman 1948). These interactions are particularly dominant at the diurnal time scale (e.g. De Bruin and Holtslag 1982) and depend on meteorological as well as on surface conditions (Jarvis and McNaughton, 1986; van Heerwaarden et al., 2010). Ignoring the interdependence of the surface variables may lead to biases in model parameterizations and compensating errors when evaluating the model performance only with respect to a single variable (Matheny et al., 2014, Best et al., 2015, Santanello et al., 2018).

There is a strong need to investigate and to derive metrics based on comprehensive observation that characterize the whole land surface-atmosphere system (Wulfmeyer et al. 2018). Several authors proposed different multivariate metrics to better evaluate land-atmosphere (L-A) interactions in observations and models. Generally, these metrics explore internal relationships between state variables to better characterize key processes and to guide a more systematic exploration and understanding of model deficiencies. A number of metrics focus on the diurnal evolution of the heat and moisture budgets in the planetary boundary layer (e.g., Betts 1992, Santanello et al. 2009, Santanello et al., 2017). Also statistical metrics exploring the strength of linear relationships between surface heat fluxes and states to surface radiation components have been employed to evaluate the performance of reanalysis with observations (Zhou and Wang 2016, Zhou et al., 2017, 2018). Furthermore, there are pattern-based metrics which focus on non-linear interactions at the diurnal time scale. Wilson et al., (2003) proposed the method of a diurnal centroid to measure the timing of the surface heat fluxes and their timing difference, which was more recently used by Nelson et al., 2018 to quantify the timing of evapotranspiration under different dryness condition for the FLUXNET dataset. In contrast Matheny et al., 2014 and Zhang et al., 2014 explored the diurnal relationship of the latent heat flux to vapor pressure deficit showing a pronounced hysteresis loop. Zheng et al., 2014 also included air temperature and net radiation as references variables and showed that the hysteresis loops of λE to D_a or T_a are large, while there are only small hysteresis effects when R_n was used. Hysteresis loops have also been found when heat fluxes plotted against net radiation (Camuffo and Bernadi 1982; Mallick et al., 2015), with many studies showing hysteretic loops of the soil heat flux against net radiation (Fuchs and Hadas, 1972; Santanello and Friedl, 2003; Sun et al., 2013). The presence of a hysteresis loop indicates that there is a time dependent non-linear control on the variable of interest, typically induced by heat storage processes. Camuffo and Bernardi (1982) showed that the magnitude

Deleted: De Bruin and Holtslag 1982) and depend on meteorological as well as on surface conditions (Jarvis and McNaughton 1986).

Deleted: To overcome these problems several authors suggested to better evaluate land-atmosphere (L-A) interactions proposing different multivariate metrics (e.g., Betts 1992, Santanello et al. 2009, Matheny et al., 2014, Zhou et al., 2016b, Santanello et al., 2017). These metrics explore internal relationships between state variables to better characterize key processes and to guide a more systematic exploration and understanding of model deficiencies. There is a strong need to investigate and to derive metrics based on comprehensive observation that characterize the whole land surface-atmosphere system (Wulfmeyer et al. 2018).¶

¶

Here, we propose an alternative metric, which focuses on the diurnal variation of surface states and fluxes with respect to incoming solar radiation (R_{sd}). It is well established that R_{sd}, which shapes the diurnal cycle of net radiation (R_n) over land, is strongly correlated with λE. Examples are

Moved down [1]: the successful application of equilibrium evapotranspiration (Schmidt 1915, Priestley-Taylor 1972, Miralles et al., 2011, Renner et al.,

Deleted: 2016), the semi-empirical Makkink equation (Makkink 1957, De Bruin and Lablans 1997, De Bruin et al., 2015) and using a fixed fraction of available energy for estimating potential evapotranspiration (Milly and Dunne 2016, Maes et al., 2018). Observations of a near linear relationship of λE to R_{sd} (Jackson et al., 1983) and the need for spatial mapping of λE stimulated remote sensing based applications (Crago, 1996). Although observations justify this simple behavior, the role of other controls on λE remains unclear (De Bruin and Holtslag 1982, Beljaars and Bosveld 1997, Best et al., 2015; Haughton et al., 2016; Zhou and Wang 2016a; Milly and Dunne 2016). This is particularly important for remote sensing based λE models since they use observational states which have an imprint of land-atmosphere interactions. ¶

¶

The relevance of other atmospheric controls on λE should result in a deviation from linearity between λE and R_{sd}. There could be a consistent lag between the diurnal patterns of λE versus R_{sd} which would reveal a loop when λE is plotted against solar radiation. There is observational evidence of such consistent loops for and direction of such hysteretic loops can be estimated by a multi-linear regression of the variable of interest against the forcing variables and its first order time-derivative. This simple model allows estimating storage effects on diurnal (Sun et al. 2013) to seasonal time scales (Duan and Bastiaansen 2017).

Deleted: to estimate

Here, we choose the Camuffo and Bernardi (1982) model because it provides an objective measure of the magnitude of hysteresis loops and it allows for an assessment of statistical significance. We extend the Camuffo and Bernardi (1982) model in two ways.
First, we use incoming solar radiation (R_{sd}) as reference variable instead of net radiation to estimate the phase lag of surface heat flux observations and models. And secondly, we use a harmonic transformation of the Camuffo and Bernardi (1982) regression model to estimate the phase lag in time units. This extension allows to compare the diurnal phase lag signatures of the different model inputs and how these influence the resulting diurnal course of the latent heat flux estimate.

Deleted: Here we use R_{sd} as independent forcing of land-atmosphere exchange to quantify the response of surface heat fluxes and states to R_{sd} as well as the magnitude and direction of phase lags. Thereby we obtain a metric to measure the influence of the various drivers of λE. Process-based models represent our knowledge of the various drivers of λE and therefore should be able to capture the magnitude of hysteretic loops under different conditions (Matheny et al., 2014). Hence, we can use the hysteretic behavior as a pattern-based approach and as an additional criterion to evaluate the performance of different models.

We specifically choose incoming solar radiation R_{sd} as the reference for the phase shift analysis, since R_{sd} can be regarded as an independent forcing of the surface energy balance (e.g. Ohmura 2014):

$$R_{sd}(1-\alpha)+R_{ld}-H-\lambda E-G=\sigma T^{4}+m \qquad (1)$$

With surface albedo α, incoming longwave radiation R_{ld}, sensible heat flux H, latent heat flux λE, the conductive soil heat flux G, the outgoing longwave radiation σT^{4} and storage terms of the surface layer summarized in m. This formulation of the surface energy balance provides the direction of the energy exchange processes at the surface, illustrating that the terms on the right-hand side depend on heat fluxes on the left-hand side of Eq. (1) (Ohmura 2014). As a consequence, the term net radiation R_n, which resembles the radiation budget of the shortwave and longwave components: $R_n = R_{sd}(1-\alpha)+R_{ld}-\sigma T^{4}$, cannot be regarded as an independent surface forcing. Consequently, we choose R_{sd} instead of R_n or R_n-G as the reference variable for the phase shift analysis of the latent heat flux and the main input variables of evapotranspiration model approaches.
We focus on two different approaches to estimate λE. The first approach is based on the energy limitation of λE, using the equilibrium evaporation concept (Schmidt 1915) as formulated by Priestley and Taylor (1972) for potential evaporation. For actual evaporation we focus on one source and two source energy balance schemes (OSEB and TSEB, respectively) which derive λE as residual term of the surface energy balance and parameterize the sensible heat flux by a temperature gradient - resistance description (Kustas and Norman 1996) (referred to as 'temperature gradient scheme'). The second approach is based on the Penman-Monteith (PM hereafter) approach (Monteith 1965), which adds water vapor pressure deficit as a driving gradient (referred to as 'vapor gradient scheme'). We use the widely used FAO Penman-Monteith formulation (Allen et al., 1998) for potential or reference evapotranspiration. For actual evapotranspiration we use a modified PM approach which was formulated by Mallick et al. (2014, 2015, 2016, 2018); (see also Bhattarai et al., 2018) and is termed as a surface temperature initiated closure (STIC). STIC is based on finding the analytical solution of the

surface and aerodynamic conductances in the PM equation while simultaneously constraining the surface and aerodynamics conductances through both surface temperature and vapor pressure deficit.

Several inter-comparison studies evaluated the performance of these schemes using observations from different landscapes. OSEB and TSEB which are often used in remote sensing retrievals of λE have been found to perform comparably well in reproducing tower-based energy flux observations (Timmermans et al. 2007; Choi et al. 2009; French et al., 2015). Yang et al. (2015) compared temperature gradient approaches (including TSEB) with the Penman-Monteith approach (based on vapor pressure gradient only) employed by the MODIS evapotranspiration product (MOD16, Mu et al., 2011) and found strongly reduced capability of MOD16 to estimate spatial variability of evapotranspiration. They concluded that the moisture availability information obtained from relative humidity and vapor pressure deficit of the air is not able to capture the surface water limitations as reflected in surface temperature.

In this study, we focus on the ability of these different evapotranspiration models to reproduce the diurnal cycle of λE under wet and dry conditions. In particular, we assess if significant non-linear relationships in form of hysteretic loops exist, if these change under different wetness conditions and if temperature-gradient and vapor-gradient approaches such as PM are able to reproduce this behavior. Further, we evaluate which input variables of the evapotranspiration schemes show a hysteretic pattern and how these patterns influence the flux estimation. To address these questions, we analyze observations and models with respect to internal functional relationships (pattern-based) and use solar radiation as independent driver of land-atmosphere exchange. We focus on wet vs. dry conditions since this is another critical deficiency identified in previous analyses (e.g. Wilson et al., 2003, Matheny et al., 2014, Zhou and Wang 2016). To ensure similar radiative forcing and avoid variability due to cloud cover we focus the evaluation on clear-sky days. We illustrate our approach on a grassland site in a temperate semi-oceanic climate using surface energy balance observations.

Deleted: et al., 2016b

The analysis will shed light on the capabilities of process-based evapotranspiration schemes to capture the dynamics of diurnal land-atmosphere exchange. We show that the phase lag of surface states and fluxes reveals important imprints of heat storage processes and how this guides the evaluation of the different approaches for modeling λE. This is important for applications in remote sensing with respect to the choice of observational input variables. In doing so, we provide a further, pattern-based metric to assess land-atmosphere interactions, and, thus guide process-based improvements and calibration of land-surface schemes.

2 Methods and Data

2.1 Diurnal patterns and hysteresis loop quantification

We first illustrate the pattern-based evaluation of the diurnal cycle using two hypothetical variables Y_1 and Y_2, as shown in Figure 1. If a variable (Y_1) is in phase with R_{sd}, it shows a linear behavior when plotted against R_{sd} (Fig. 1 b). However, if a variable (Y_2) has a time lag with respect to R_{sd}, showing a significant difference between morning and afternoon values, it results in a hysteretic loop. The area inside the loop indicates the magnitude of the phase difference, while the direction of the loop, marked by an arrow at the morning rising limb in Fig. 1b, indicates if a variable is preceding or lagging R_{sd} in time. If a variable shows consistently larger values during the afternoon as compared to the morning, this will appear as a counter-clockwise (CCW) hysteretic loop indicating a positive phase lag with respect to R_{sd}. A negative phase lag appears as a clockwise (CW) loop.

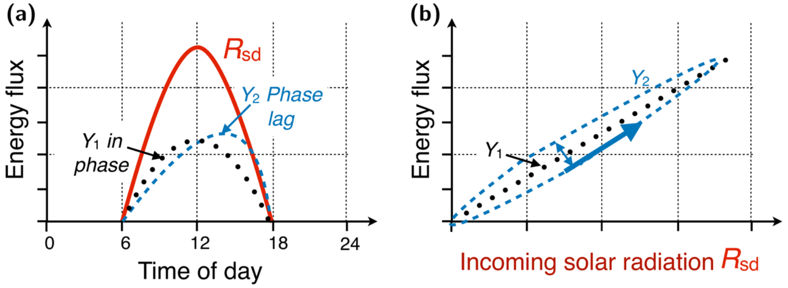

Figure 1: Illustration of a pattern-based evaluation of the diurnal cycle. Panel a) shows the diurnal cycle of R_{sd} under clear-sky conditions and the diurnal cycle of two variables Y_1 and Y_2, one in phase with R_{sd} and another lagging R_{sd}. Panel b) illustrates the relationship of these variables when plotted against R_{sd}. The bold arrow indicates the direction of the loop and the area inside the hysteresis describes the magnitude of the phase shift.

To obtain a quantitative measure of the hysteretic pattern, we use the Camuffo-Bernardi equation (Camuffo and Bernardi 1982), which relates the time series of the response variable $Y(t)$ to the forcing variable $R_{sd}(t)$ and its first order time derivative $dR_{sd}(t)/dt$:

$$Y(t) = a + b\,R_{sd}(t) + c\,(dR_{sd}(t)/dt) + \varepsilon(t). \qquad (2)$$

Deleted: →(1

Using multi-linear regression, we obtain the coefficients a, b and c assuming a normal distribution of the residuals $\varepsilon(t)$. If Y is linear with R_{sd}, the parameter c should be zero. However, if a consistent pattern such as a hysteretic loop exists, then parameter c should be significantly different from zero. Hence, by using regression analysis we can determine if a significant hysteretic relationship between two variables exists, and if the inclusion of such a non-linear term (with $c \neq 0$) would improve the model fit.

Although significance testing of the coefficient c is an advantage, it is clear from Eq. (2) that the magnitude of c depends on the units and magnitude of the response variable Y. In order to estimate a comparable estimate of the phase lag we employ a harmonic transformation of the regression model. Assuming that R_{sd} is a harmonic function with an angular frequency ω, the phase difference φ can be estimated from the two regression coefficients b and c:

Deleted: Both,

Deleted: parameters *b* and

Deleted: contain information

Deleted: between the two variables.

Deleted: by

$$\varphi = \tan^{-1}(c\ \omega / b) \qquad (3)$$

Deleted: 2

To derive the first order time derivative of solar radiation, we use a simple difference between time steps. Since the data we use is available in 30 min time steps (see below), we have 48 time steps per day, thus $\omega = 48/(2\pi)$. To obtain a phase lag between Y and R_{sd} as a time lag t_φ [min] we use:

$$t_\varphi = \tan^{-1} (48/(2\pi)\ \ c / b)\ (60 \times 24/(2\ \pi)). \qquad (4)$$

Deleted: (3

Note that the phase lag estimate t_φ is somewhat similar to the relative diurnal centroid metric proposed by Wilson et al., (2003) for the analysis of the timing of heat and mass fluxes. The diurnal centroid identifies the timing of the peak of a variable with respect to local time. Since the peak of R_{sd} is at noon local time both metrics are qualitatively comparable.

2.2 Field site and observations

The study area is a grassland site in Petit-Nobressart, Luxembourg, situated on a gentle east facing slope. The grassland is used as a hay meadow and had short vegetation of about 10-15 cm as the grass was mowed before the start of the experiment. An Eddy-Covariance (EC) station (with the setup described in Wizemann et al. 2015) was installed at the grassland close to the village of Petit Nobressart (Fig. 2, exact coordinates: N 49° 46.77’ E 05° 48.22’). The EC station was operated from 11 June until 23 July 2015. The three-dimensional wind and temperature fluctuations were measured at 2.41 m above ground by a sonic anemometer (CSAT3, Campbell Scientific Inc., Logan, USA) facing to the mean wind direction of 290°. A fast response open-path CO2/H2O infrared gas analyzer (IRGA LI-7500, LI-COR, USA) installed in a lateral distance of 0.2 m to the sonic path was used to measure CO2 and H2O fluctuations. The high-frequency signals were recorded at 10 Hz by a CR3000 data logger and the TK3 software was used to compute turbulent fluxes of sensible heat (H), latent heat (λE) and CO2 (Mauder and Foken, 2015).

Downwelling and upwelling shortwave and longwave radiation were obtained by a four-component net-radiation sensor (NR01, Hukseflux, Netherlands). The meteorological variables (air temperature, humidity and precipitation) were monitored with a time resolution of 30 minutes. Soil heat flux was measured by heat flux plates (two in 8 cm depth, HFP01, Hukseflux, Netherlands), soil temperature (2, 5, 15, 30 cm, model 107, Campbell Scientific Inc., UK), water content (2.5, 15, 30 cm, CS616, Campbell Scientific Inc., UK) and matric potential (5, 15, 30 cm, model 253, Campbell Scientific Inc., UK) were installed between the turbulence and radiation measurement devices.
Unfortunately, the two upper temperature probes and soil matric potential sensors showed data gaps and erroneous values from 30 June until excavation on 23 July, 2015. Thus, the ground heat flux was calculated by the heat flux plate method with correction for heat storage (Massman, 1992) only for the period from 11 June to 30 June, 2015. To still obtain soil heat fluxes for the entire measuring period, additionally harmonic wave analysis (Duchon and Hale, 2012) of the heat flux plate data was applied. The harmonic wave analysis calculates the wave spectrum at the soil surface from the Fourier transform of the soil heat flux measured by the heat flux plates in a few cm depth (here: 8 cm) by correcting for wave amplitude damping and phase shift. The surface ground heat flux is then obtained by an inverse Fourier transformation of the corrected wave spectrum. The method has a dependence on soil moisture

Deleted: Sensors measuring soil

Deleted:)) of the heat flux plate data was applied. Both methods affecting the damping depth. The dependence is, however, weak for clayey soils with soil water contents > 10% (Jury and Horton 2004) as observed at the site. The damping depth was obtained by the exponential decay of the soil temperature amplitude measured at the various depths. Differences in the damping depth between wet and drier soil moisture conditions only yielded differences in *G* smaller than 10 W m^{-2}. Therefore, we used a constant damping depth for the whole period.

Both methods for deriving the total soil heat flux agreed well for the period before 30 June, so that the latter method should provide reliable ground heat flux values for the entire period until 23 July. Table 1 lists the variables obtained from the EC station and used in this work. For more details on instrumentation and EC data processing see Ingwersen et al. (2011) and Wizemann et al. (2015).

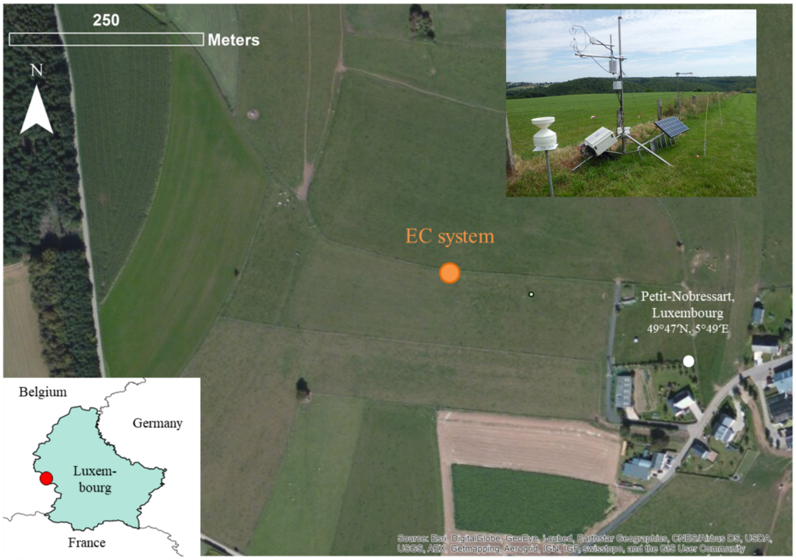

Figure 2: Location of the EC site at Petit-Nobressart, Luxembourg. Top right inset shows the mast with sonic anemometer and infrared gas sensor (center), radiation sensor (right) and rain sensor (left). The soil sensors are located on the right of the solar panel. Photo: Elisabeth Thiem. Background: ESRI ® World Imagery.

2.2.1 Derived meteorological variables

We derived the saturated water vapor pressure e_s (hPa) by the empirical Magnus equation (Magnus 1844) as a function of air temperature T (°C) with empirical coefficients from (Alduchov and Eskridge, 1996):

Deleted: We derived the saturated water vapor pressure e_s (hPa) by the empirical Magnus equation (Magnus 1844) as a function of air temperature T (°C):¶
¶

$$e_s\,(T) = 6.1094 \text{ hPa } e^{(17.625\, T\,/\,(243.04\, +\, T))}$$

Deleted: 1078

Deleted: 08085

Deleted: 234.175

Then, the water vapor pressure of the air e_a (hPa) was obtained by using air temperature T_a and relative humidity (r_H):

$$e_a = e_s\,(T_a)\; r_H/100.$$

To assess the moisture conditions of each date of the site we used the evaporative fraction f_E:

$$f_E = \lambda E\,/\,(H + \lambda E).$$

Since daily averages can be influenced by single large values of the turbulent fluxes and contain missing values, we estimated a daily f_E based on the 30 min values of each day using the following linear regression:

$$\lambda E = f_E\,(H + \lambda E) + \beta + \varepsilon_R$$

Deleted: α

where f_E is the slope of the linear regression, β its intercept and ε_R the residuals. Since we use the fluxes of H and λE without energy balance closure correction we obtain the upper range of f_E.

Deleted: α

Since the sonic anemometer measures friction velocity (u^*) and the absolute value of wind speed $u = sqrt(U^2+V^2)$, we estimate the aerodynamic conductance for momentum (u^{*2}/u) and the aerodynamic conductance (g_{ah}) for heat including the excess resistance to heat transfer using an empirical formula by Thom (1972):

$$g_{\mathrm{ah,Thom}} = \left(\frac{u}{u^{*2}} + \frac{6.2}{u^{*\frac{2}{3}}}\right)^{-1} \qquad (5)$$

Deleted: →(4

We chose to use this formula for its simplicity and similar performance than more recent, complex parameterizations (Knauer et al., 2018, Mallick et al. 2016). Also note that effects of atmospheric stability are accounted for in the first term of Eq. (5).

Deleted:).

Deleted: 4

2.2.2 Energy balance closure gap correction

Most EC measurements show that the sum of the observed turbulent heat fluxes are smaller than the available energy and thus do not close the energy balance leaving an energy balance closure gap (Q_{gap}) (Foken et al., 2008)

$$Q_{\mathrm{gap}} = R_{\mathrm{n}} - (G + H + \lambda E)$$

For our site we observed on average a slope of $(H + \lambda E) \sim (R_{\mathrm{n}} - G) = 0.81$ (by linear regression) with an average gap of 37 W m^{-2} over the whole duration of the field campaign. These values are in the typical range what is commonly found for grassland sites (Stoy et al., 2013).

Deleted: /

Commented [MR1]: I found a typo the average gap is 37 W/m2

Deleted: 67

To correct the turbulent fluxes for the energy balance closure gap (evaluated at the 30 min time steps), we use a correction based on the Bowen ratio (B_{R}) (Twine et al., 2000), which is directly related to the evaporative fraction $f_{\mathrm{E}} = 1/(B_{\mathrm{R}}+1)$ to obtain corrected fluxes:

Deleted: ,

$$\lambda E_{\mathrm{BRC}} = \lambda E + Q_{\mathrm{gap}} * f_{\mathrm{E}}$$

and

$$H_{\mathrm{BRC}} = H + Q_{\mathrm{gap}} * (1-f_{\mathrm{E}})$$

Thereby, we used the daily f_{E} estimate. We use these corrected fluxes in the further analysis.

2.2.3 Clear-sky day classification

In order to achieve comparable conditions with respect to incoming solar radiation, we identified clear-sky conditions. A clear-sky day was defined by its daily sum of incoming solar radiation being larger than 85% of the potential surface radiation ($R_{\mathrm{sd,pot}}$), which is a function of latitude and day of year (using R package REddyProc, function fCalcPotRadiation):

$$R_{\mathrm{sd}}/ R_{\mathrm{sd,pot}} > 0.85 \quad \Sigma(R_{\mathrm{sd}}(t)) / \quad (f_{\mathrm{diff}}\, \Sigma(R_{\mathrm{sd,pot}}\,(t))),$$

where t corresponds to each time step of measurement and $f_{\mathrm{diff}} = 0.78$ being a constant factor taking account for atmospheric extinction of solar radiation.

Deleted: absorption

2.3 One and Two Source Energy Balance models

Thermal remote sensing based models estimate evapotranspiration by solving the surface energy balance and rely on land surface temperature (T_{s}) information as a key boundary condition (Kustas and Norman 1996). A bulk layer formulation of the soil-plus-canopy sensible heat flux is employed and λE is derived by enforcing the surface energy balance. Hence λE is written as:

$$\lambda E = R_n - G - H = R_n - G - \rho\, c_p\, (T_s - T_a)\, g_{ah}, \qquad (6)$$

Deleted: (5

where ρ is density of air, c_p is the specific heat of air at constant pressure, and g_{ah} is the effective aerodynamic conductance of heat that characterizes the transport of sensible heat between the surface and the atmosphere. We obtained T_s from the observed longwave emission of the surface $T_s = (R_{lu}/(\sigma\, \varepsilon_s))^{1/4}$ with $\sigma = 5.67 \times 10^{-8}$ W K^{-4} the Stefan Boltzmann constant and a surface emissivity $\varepsilon_s = 0.98$, which is typical for a grassland and agrees with Brenner et al., (2017).
We use two different approaches which are generally classified as one- and two-source models with regard to the implemented treatment of the energy exchange with the surface. While one-source energy balance models (OSEB) treat the surface as a uniform layer, two-source energy balance models (TSEB) partition temperatures, radiative and energy fluxes into a soil and vegetation component. The one-source approach (OSEB) parameterizes the aerodynamic conductance g_{ah} as follows (e.g. Kalma et al., 2008, Tang et al., 2013):

$$g_{ah,\mathrm{OSEB}} = \frac{k^2 u}{[\ln((z_u - d)/z_{0m}) - \Psi_m]\,[\ln((z_t - d)/z_{0m}) + \ln(z_{0m}/z_{0h}) - \Psi_h]} \qquad (7)$$

Deleted: (6

where z_u and z_t are the measurement heights of wind and air temperature, respectively, z_{0m} and z_{0h} are roughness lengths for momentum and heat, respectively, k is the von Kármán constant, d is the displacement height, u is the wind speed and Ψ_m and Ψ_h are the the integrated Monin-Obukhov (MO) similarity functions which correct for atmospheric stability conditions (Brutsaert 2005, Jiménez et al., 2012). For the investigated grassland site, d and z_{0m} were calculated as fractions of the vegetation height, h_c, with $d = 0.65\, h_c$ and $z_{0m} = 0.125\, h_c$. The roughness length for heat z_{0h} was set using the dimensionless parameter $kB^{-1} = \ln(z_{0m}/z_{0h})$, which was set to 2.3 in accordance with Bastiaanssen et al., 1998. Note that this parameterization of aerodynamic conductance does not explicitly distinguish between bare soil and canopy boundary layer conductance, as it is done in two-source approaches.

In addition to OSEB we applied the Two-Source Energy Balance (TSEB) model developed by Norman et al., (1995), Kustas and Norman (1999). For both, the soil and canopy components a separate energy balance (with different component temperatures) and bulk resistance scheme with different aerodynamic conductance are formulated. Then the energy balance equations are solved iteratively. It starts by assuming that a fraction of the canopy (described by vegetation greenness fraction f_g) transpires at a potential rate as described by the Priestley-Taylor equation (Priestley and Taylor 1972):

$$\lambda E_{PT} = \alpha_{PT} \frac{s}{s+\gamma} (R_n - G) \qquad (8)$$

Deleted: R_n (7

where α_{PT} is the Priestley-Taylor coefficient (1.26), s is the slope of the saturation water vapor pressure curve and γ is the psychrometric constant. However, the canopy latent heat flux $\lambda E_c = f_g\, \lambda E_{PT}$ might be too large and the soil component would become negative (condensation at the soil surface) which is unlikely during daytime conditions. To avoid condensation at the soil surface, the α_{PT} coefficient is reduced incrementally until the soil latent heat flux becomes zero or positive. Once this condition is met, all other energy balance components are updated accordingly to satisfy the energy balance equation. For this study we used a constant vegetation fraction of $f_c = 0.9$ and a greenness fraction f_g which was derived from close-up pictures taken at the beginning and the end of the field campaign and linearly interpolated in-between.

2.4 Penman-Monteith approach

In the Penman-Monteith approach (Monteith 1965) the inclusion of physiological conductance (g_s) imposes a critical control on λE:

$$\lambda E = \frac{s\,(R_n - G) + \rho\, c_p g_{av}(e_s(T_a) - e_a)}{s + \gamma(1+\frac{g_{av}}{g_s})} \qquad (9)$$

Deleted: (8

In equation (8), the transfer of moisture is linked to a supply-demand reaction where the net available energy ($R_n - G$) is the supplies the energy for evaporation and the vapor pressure deficit of the air, D_a [$= e_s(T_a) - e_a$] is the demand for evaporation from the atmosphere. In the PM approach, the two conductances, the aerodynamic conductance g_{av} and the surface conductance g_s to water vapor are unknown. A widely used approach to obtain a reference evapotranspiration estimate from meteorological data is the FAO Penman-Monteith reference evapotranspiration (Allen et al., 1998). It defines the two conductances for a well-watered grass surface with a standard height of $h = 0.12$ m. The aerodynamic conductance is obtained by a bulk approach (eq. 7) with wind speed u measured at 2m above the surface, $d = ⅔\,h$, $z_{0m} = 0.123h$, $z_{0h} = 0.1z_{0m}$ yielding $g_{av} = u/208$ (Box 4 in Allen et al., 1998). Surface conductance is fixed at a constant $g_s = 1/70$ *m/s*. Here, we use the latter definitions of the conductances and use direct measurements for the other input variables of equation (9) to obtain the FAO Penman-Monteith estimate. While the FAO estimate is typically intended for estimates of the reference evaporation for well-watered grass on a daily basis, we use it here as a reference for comparison on a sub-daily scale. In order to understand the effect of the aerodynamic conductance parameterizations we add another reference evapotranspiration estimate in which the aerodynamic conductance is given by eq. (5) using observations of friction velocity and wind speed, but keeping g_s fixed.

Deleted: 6

Deleted: subdaily

Deleted: 4

2.4.1 Penman-Monteith based Surface Temperature Initiated Closure (STIC) (version STIC1.2)

In order to estimate an actual evapotranspiration rate from meteorological data we employ a method (STIC1.2 hereafter referred to as STIC), which is based on the PM equation, but which in addition integrates surface temperature information. The STIC methodology is based on finding analytical solutions for the two unknown conductances to directly estimate λE (Mallick et al., 2016, 2018). STIC is a one-dimensional physically-based SEB model that treats the vegetation-substrate complex as a single unit (Mallick et al., 2016; Bhattarai et al., 2018). The fundamental assumption in STIC is the first order dependency of g_a and g_s on soil moisture through T_s and on environmental variables through T_a, D_a, and net radiation. Thereby, surface temperature is assumed to provide information on water-limitation which is linked to the advection-aridity hypothesis (Brutsaert and Stricker 1979). In STIC, no wind speed is required as input data, as opposed to the temperature gradient approaches, but vapor pressure of the air and its saturation value become critical input variables, see Table 2 for an overview.

A detailed description of STIC version 1.2 is available in Mallick et al. (2016, 2018) and Bhattarai et al. (2018).

3 Results

3.1 Daily clear-sky and moisture classification

The field campaign was conducted during an exceptionally warm and dry period characterized by clear sky conditions with remarkably high air temperatures with daily maxima above 30°C and little precipitation. Compared to the climatic normal (1981-2010) the precipitation deficit in this region was -44% in June and -41% in July, respectively (source: meteorological station Arsorf, Administration des services techniques de l'agriculture (ASTA)). The air temperature anomaly was higher in July (1.9°C) than in June (0.7°C) (source: meteorological station Clemency, ASTA). The soil water content decreased and parts of the site, especially in the upper part, showed clear signs of vegetation water stress (see Brenner et al., (2017) for an analysis of the spatial heterogeneity of water limitation). However, the dry period was interrupted by a few but strong rainfall events, which significantly changed soil moisture and thus f_E with time (Fig. 3a). Based on the observed f_E we classified dry days with $f_E < 0.5$ and wet days with $f_E > 0.6$. This separation of dry and wet days is also reflected in the top soil moisture conditions (measured at 5 cm depth) as shown in Fig 3b.

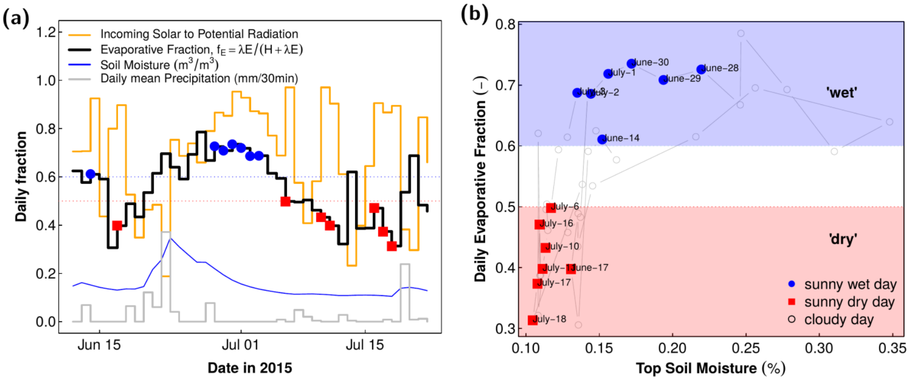

Figure 3: Daily observations of soil moisture, evaporative fraction, ratio of observed to potential solar radiation and mean precipitation. Panel a) shows the daily time series and panel b) the relationship of f_E to soil moisture used to classify "wet" and "dry" days depending on $f_E > 0.6$ or $f_E < 0.5$, respectively. Sunny days are defined using a threshold of 85% of R_{sd} to potential radiation and are marked with solid symbols, with blue circles referring to wet and red squares to dry days. Top soil moisture measured at 5 cm below surface is shown.

Based on the classification into wet and dry days under clear-sky conditions we computed composites of the diurnal cycle for each hour. By using only sunny days we aim to achieve similar conditions with respect to downwelling shortwave radiation (R_{sd}). Figure 4a confirms that R_{sd} and net radiation (R_{n}) had very similar diurnal cycles and magnitudes for the wet and dry days. However, the downwelling longwave radiation R_{ld} and the soil heat flux were somewhat higher under wet conditions (Fig. 4a). The higher R_{ld} is related to a higher air temperatures and air vapor pressures observed under wet conditions (Fig. 4b), which may explain the greater value of R_{ld} by affecting the atmospheric emissivity for longwave radiative exchange. This has also an impact on the minimum temperatures both for air and skin temperature, which are higher under wet conditions and lower under dry conditions (Fig. 4b). Hence, although we achieve fairly similar conditions for shortwave radiation under wet and dry conditions, we observed a small but significant difference in the longwave radiative exchange.

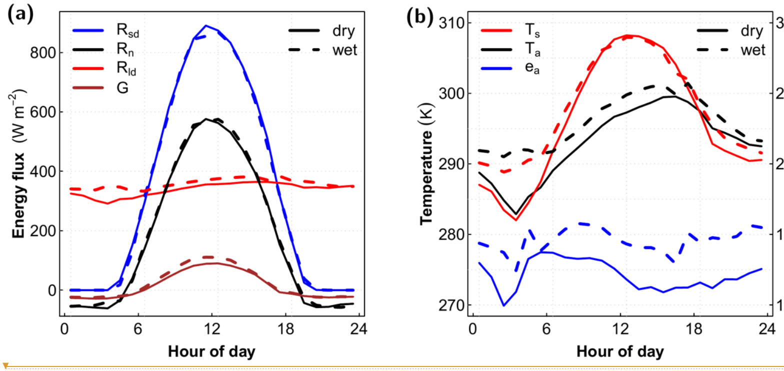

Figure 4: Observations of average diurnal cycles of energy fluxes (panel a, with R_{sd}: shortwave downwelling flux, R_{ld}: longwave downwelling flux; R_{n}: net radiation; G: ground heat flux); surface and air temperatures, T_s and T_a, and air vapor pressure, e_a, (panel b) comparing wet and dry days.

3.2 Diurnal cycle of evapotranspiration under wet and dry conditions

Next, we evaluate how the different evapotranspiration schemes are able to reproduce the fluxes during wet and dry conditions under similar R_{sd} forcing. Figure 5 shows the average diurnal cycle of observations and models for λE. The observations showed a significant difference in λE between dry and wet conditions, with the maximum value of λE of about 200 W m^{-2} for dry and 350 W m^{-2} under wet conditions, which amounts to a mean difference of 100 W m^{-2} for daylight conditions (Table 3). As reference, we also included two common formulations of potential evapotranspiration, the Priestley-Taylor potential evapotranspiration (PT) and the FAO Penman-Monteith reference evapotranspiration (FAO-PM). Both do not account for water limitation and show a marginal difference of 10 W m^{-2} between wet and dry conditions. While FAO-PM yielded lower mean conditions than PT, it showed lower correlation and RMSE as compared to PT (Table 3). We find that all models for actual λE (rather than PT or FAO-PM) showed differences in λE between wet and dry conditions. Both OSEB and TSEB

Deleted:

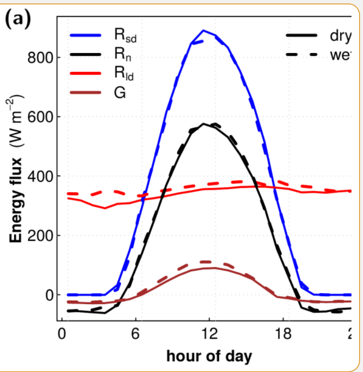

showed a tendency to overestimate λE under dry conditions but captured the high λE values under wet conditions. In contrast, STIC captured the low λE magnitude under dry conditions (f_E<0.5) but underestimated λE under wet conditions (for f_E>0.6).

Table 3 shows the statistical metrics of the model performances with respect to the Bowen ratio corrected λE. In general, both OSEB and TSEB produced mean λE values within the range of 96 - 98% (255 W m^{-2} and 259 W m^{-2}) of the observed λE (264 W m^{-2}) in wet conditions, while mean λE from STIC was within 83% (218 W m^{-2}) of observed λE for the same conditions. However, for the dry conditions, simulated λE from STIC (180 W m^{-2}) was 91% of the observed mean λE (164 W m^{-2}), while the simulated mean λE from OSEB and TSEB was 77 - 78% of the observed mean λE. Overall, the three models captured 86% (OSEB), 88% (TSEB), and 95% (STIC) of the observed mean λE. Results show that under wet conditions, RMSE of the OSEB /TSEB models is well within the range of the errors when compared with the uncorrected λE, whereas STIC showed relatively higher RMSE. However, under dry conditions the RMSE of OSEB /TSEB models was found to be larger than for STIC. For the entire observation period the three models produced comparable RMSE (41 - 46 W m^{-2}) but with different correlation. STIC produced relatively low correlation ($r^2 = 0.72$) as compared to the other two models ($r^2 = 0.84 – 0.85$). Thereby, we find that the correlation of the schemes is distinctly larger under wet conditions as compared to dry conditions. The correlation under wet conditions of OSEB and TSEB are in the range of the correlation of the uncorrected λE ($r^2 = 0.91$), whereas STIC and FAO-PM showed lower correlation. Under dry conditions the correlation was significantly lower than the correlation of the uncorrected λE ($r^2 = 0.93$). While OSEB/TSEB explained 62% of the observed uncorrected λE variability in dry conditions (STIC explained 44%), both models produced higher RMSE (57 - 58 W m^{-2}) as compared to STIC (45 W m^{-2}) under these conditions.

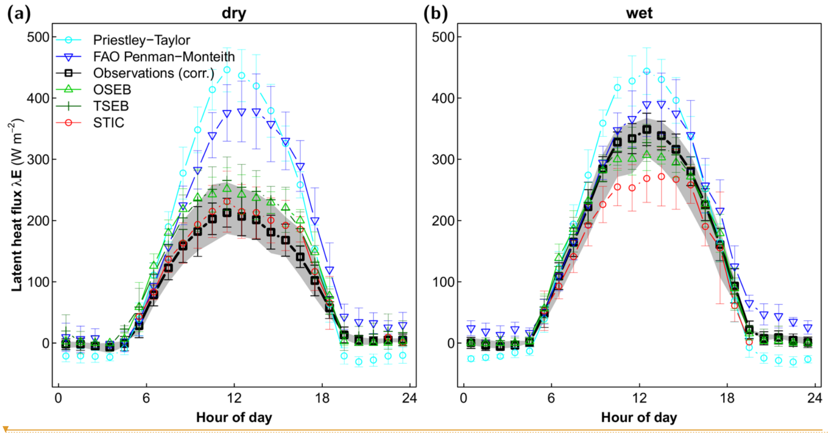

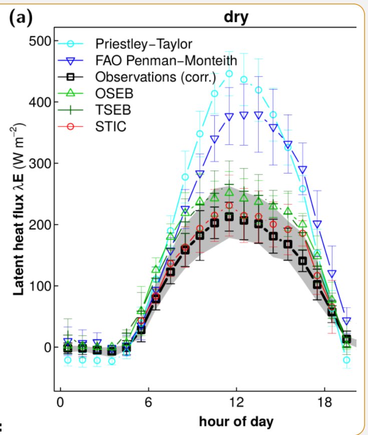

Deleted:

Figure 5: Average diurnal cycle of λE estimates for (a) dry and (b) wet days. Error bars denote the standard deviation obtained for each hour. The bold black line with squares shows the observed latent heat flux corrected for the surface energy balance closure (λE_{BRC}). The grey-shaded area depicts the range induced by the energy balance closure gap.

3.3 Diurnal patterns of evapotranspiration

The evaluation of the diurnal cycle shows that λE was strongly related to the incoming solar radiation, emphasizing that R_{sd} is the dominant driver of λE (Fig. 6). However, under wet conditions we found a marked and consistent difference between morning and afternoon in λE forming a CCW hysteresis loop (Fig. 6b). Using the Camuffo-Bernardi regression we found a significant phase lag for the BR corrected flux (λE_{BRC}) with a mean t_φ = 15 min under wet conditions and no significant lag under dry conditions (Fig. 7 and Table 4). The uncorrected observations showed only a slightly lower wet-dry difference highlighting that the method to close the energy balance closure gap does not significantly influence the estimated phase lag.

Deleted: .

The two potential evapotranspiration estimates showed large differences in their phase lag. While the PT estimate showed a small hysteretic loop with a phase lag between t_φ = 6-9 min, the FAO-PM estimate showed a substantial loop with a phase lag of t_φ = 31 min. This large phase lag of the FAO-PM estimate is very similar to the phase lag when we use a constant g_s in the PM equation but with g_{av} obtained from Eq. (5) using friction velocity observations (Table 4). The temperature gradient schemes (OSEB and TSEB) reproduced the observed phase lag relatively well (mean t_φ = 9 min for wet and around 0 for dry conditions). However, the temperature-vapor gradient scheme (STIC) showed relatively larger phase lags under both dry and wet conditions (t_φ = 14-20 min) (Fig. 7, Table 4).

Deleted: 4

Since all evapotranspiration schemes use R_n-G as forcing, we also computed the phase lags with R_n-G as a reference variable (see Table 4). The differences to R_{sd} as reference are, however, rather small with slightly lower phase lags and in the range of the standard deviation of the daily estimates. This small difference can be attributed to a negligible phase lag between R_{sd} and R_n as well as the rather small magnitude and the phase lag of the soil heat flux.

Deleted:

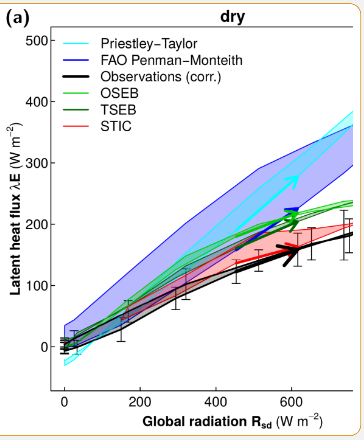

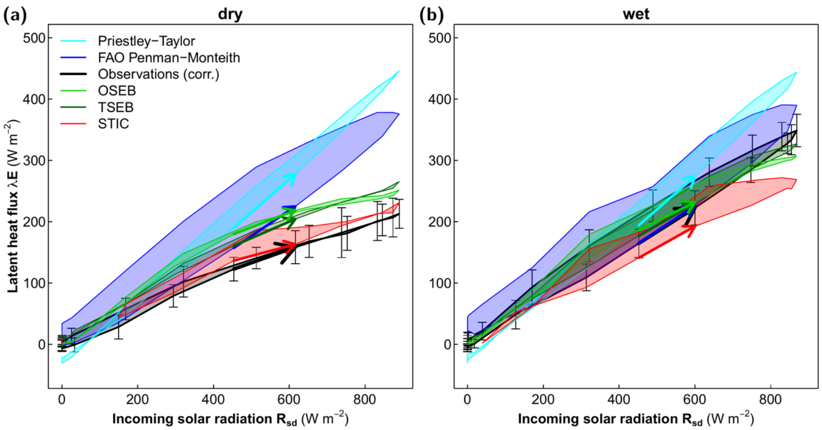

Figure 6: Diurnal hysteresis of λE to R_{sd} for (a) dry and (b) wet conditions of observations and different models. Bold arrows indicate the rising limb in the morning hours (7:00 to 8:00) showing a counterclockwise hysteresis of λE under wet conditions. Vertical arrows depict the standard deviation of λE_{BRC} for each hour.

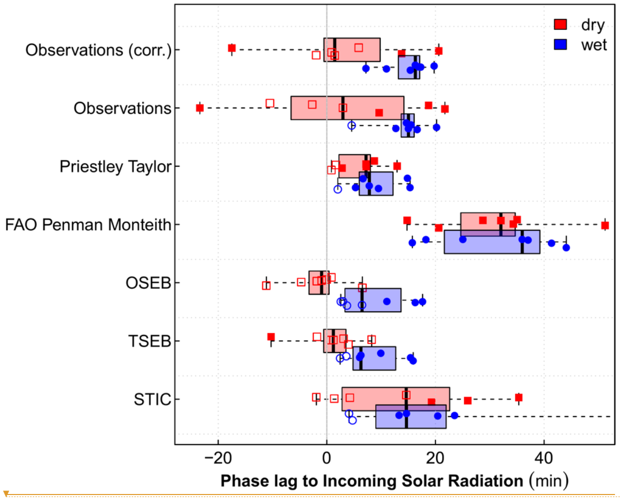

Figure 7: Boxplot of the daily phase lag of λE to R_{sd} for observed (without and with Bowen Ratio correction) and modeled latent heat flux using sunny, dry (red) and wet (blue) days. A positive phase lag means that λE follows R_{sd}, and thus forms a CCW hysteresis as shown in Fig. 6. Dots show the actual data for each day with filled symbols indicating significant phase lags ($P < 0.05$, t-test of coefficient significantly different from 0).

Deleted:

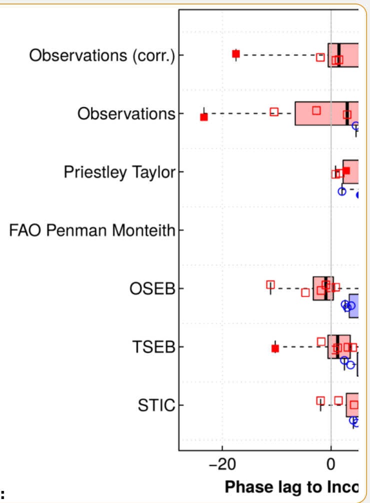

3.4 Diurnal patterns of observed fluxes and states

In order to understand the diurnal patterns of λE we also analyzed the hysteresis loops of the observed surface energy balance components [$\lambda E = (R_n - G) - H$] with respect to R_{sd} (Figure 8). Generally, there was only a small hysteresis in the available energy ($R_n - G$) (Table 4). The turbulent heat fluxes showed significant hysteresis under wet conditions but not under dry conditions. Interestingly, under wet conditions the CCW hysteresis of λE with a phase lag (mean $t_{\varphi} = 15$ min) was mostly compensated by a CW hysteresis of H (mean $t_{\varphi} = -22$ min) (Figure 8 and Table 4). This compensation is an outcome of net available energy ($R_n - G$) showing little hysteresis for both conditions.

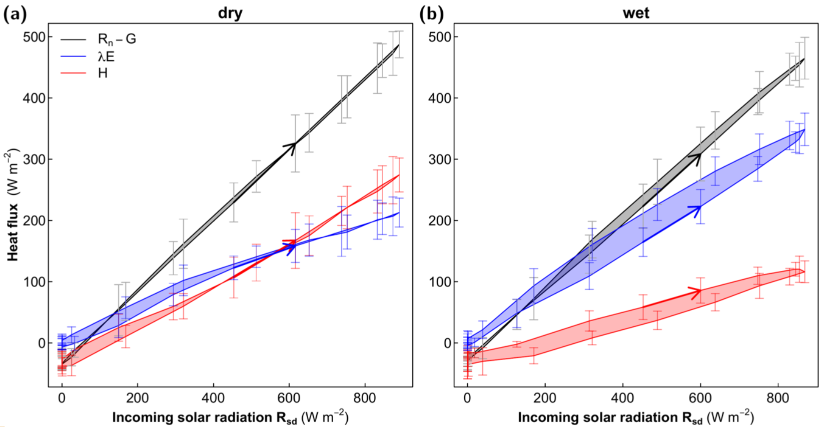

Figure 8: Diurnal patterns of observed surface energy balance components for (a) dry and (b) wet days. The lines show the composite average and vertical bars the standard deviation for available energy (black), latent (blue) and sensible heat (red) of each hour. There is a nearly linear response of all surface heat fluxes to R_{sd} under dry conditions, and a systematic hysteresis loop under wet conditions. Under wet conditions the CCW hysteresis of λE is mostly compensated for by a CW hysteresis of H.

We next analyzed the bulk sensible heat flux formulation used in the OSEB and TSEB models to understand how the observations of temperature and the inferred aerodynamic conductances are related to each other. The diurnal patterns of both air and surface temperature revealed a strong CCW hysteresis with R_{sd} (Fig. 9). Air temperature showed a more pronounced hysteretic loop than surface temperature, and with a triangular shape with higher values during the afternoon when solar radiation reduces. Interestingly, the surface-air temperature gradient, being the driving gradient for the sensible heat flux,

Deleted:

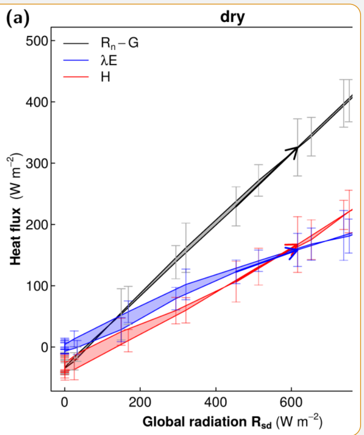

showed much less hysteretic behavior. The hysteresis is in a clockwise direction, with a higher gradient in the morning hours compared to the afternoon. It had a similar phase lag as H (see Table 4).

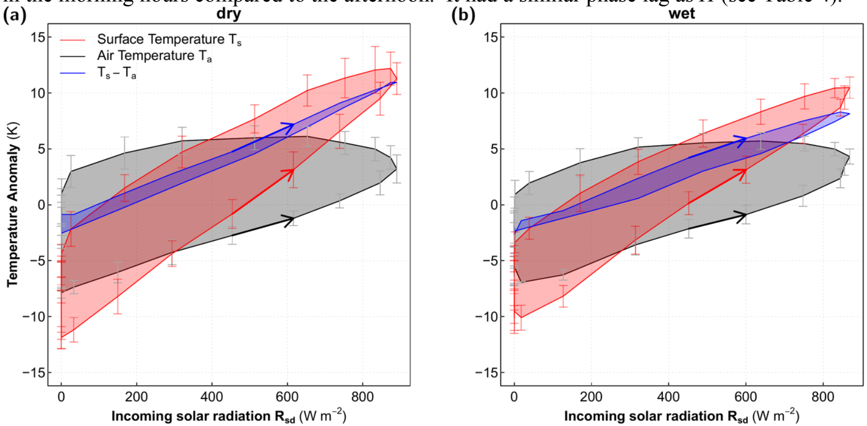

Figure 9: Diurnal patterns of observed anomalies in surface temperature (T_s), air temperature at 2m (T_a), and their gradient (T_s – T_a) for (a) dry and (b) wet days. Both T_a and T_s show a pronounced CCW hysteresis, but the form of the hysteretic loop is significantly different, with air temperature featuring a more pronounced, triangular shape with afternoon values almost independent of incoming solar radiation. The temperature gradient, however, shows a much smaller CW hysteretic loop. Note that the temperature gradient is comparatively higher in the morning than in the afternoon, corresponding to the diurnal course of the sensible heat flux (cf. Fig. 8).

We further analyzed different formulations of the aerodynamic conductance (g_a) directly inferred from measurements and from how these are represented in the models evaluated here (FAO-PM, OSEB, TSEB, STIC). We inferred the aerodynamic conductance from observations in three different ways: Firstly, we used the Eddy-Covariance measurements of friction velocity (u^*) and wind speed (u) to estimate the aerodynamic conductance for momentum ($g_{am} = u^{*2}/u$). We then used the empirical formula by Thom (1972) to calculate the aerodynamic conductance for heat including the excess resistance to heat transfer (Eq. 5). Thirdly, we inferred the aerodynamic conductance from the observed sensible heat flux (H_{BRC}) and temperature gradient (T_s - T_a) by inverting H_{BRC} using Eq. (6). The FAO-PM describes the aerodynamic conductance with a simple linear relationship to wind speed. OSEB and TSEB estimates the aerodynamic conductance to heat (g_{ah}), while STIC estimates the conductance to water vapor (g_{av}). Thus by comparing these different conductance estimates we assume similarity between the fluxes.

The different estimates for the aerodynamic conductance are compared to each other in Fig. 10 for midday conditions. Although the three observation-based estimates show some variations in the absolute value of the aerodynamic conductance, they consistently showed a significantly greater conductance for dry days compared to wet days, suggesting a stronger aerodynamic exchange between

Deleted:

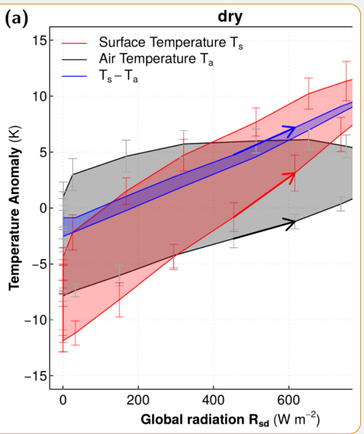

Deleted: covariance

Deleted: 4

Deleted: 5

Deleted: conducatance eatimates

the surface and the atmosphere under dry conditions. This difference in aerodynamic conductance is partly reproduced by the simple FAO-PM scheme which means that the median wind speed was higher under the drier conditions. The temperature-gradient schemes (OSEB and TSEB) reproduce the wet-dry difference rather well, which also use wind speed but rely on MOST similarity and stability correction. STIC which does not use wind speed did not show any significant differences in g_{av} between wet and dry conditions.

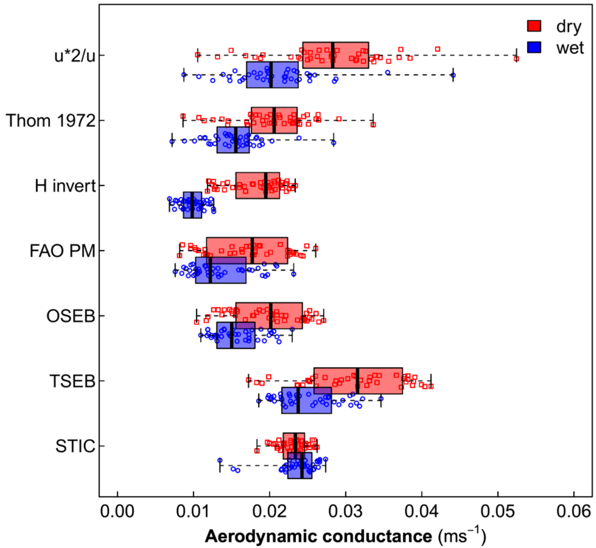

Figure 10: Boxplot of the different estimates of aerodynamic conductance under dry (red) and wet (blue) conditions. Only sunny days are sampled and midday values (10:00-15:00) are used in the comparison. The top three estimates are directly inferred from observations, as described in the text.

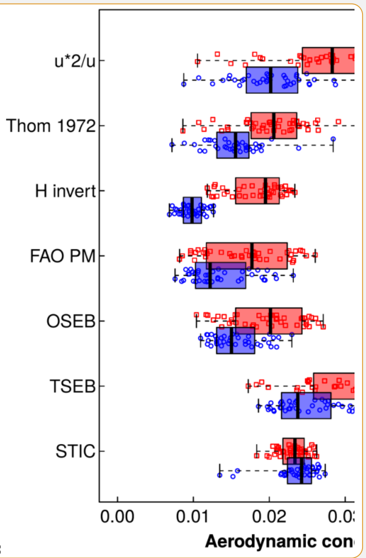

Deleted:

Finally we analyze the diurnal patterns of the vapor pressure deficit $D_a = e_s(T_a) - e_a$ which is a critical driver of the latent heat flux in the PM equation. Since D_a is derived from the observations, we analyzed its diurnal patterns in Fig. 11. We found that the vapor pressure in the air remained fairly constant during the day, hence it did not co-vary with R_{sd}, and only showed a small CW hysteresis with higher vapor pressure during the morning than during the afternoon. The saturation vapor pressure, which is a function of air temperature, however, showed a distinct and large CCW hysteresis loop with respect to R_{sd}, which is consistent with the large hysteresis in air temperature (Figs. 9 and 12). As a consequence, D_a also showed a distinct and large CCW hysteresis with a large phase lag of t_φ=~ 150 min (see Table

4). This large hysteresis and phase lag is consistent with the respective characteristics of air temperature, but not with those of the temperature gradient, cf. Fig 9. Furthermore, we note that the phase lag in D_a did not show any significant influence of wetness, while the phase lag of the temperature gradient became more negative under wet conditions (Fig. 12, Table 4). It would thus seem that the bias in PM-based estimates identified here may relate to a too pronounced role of D_a in the evapotranspiration estimate.

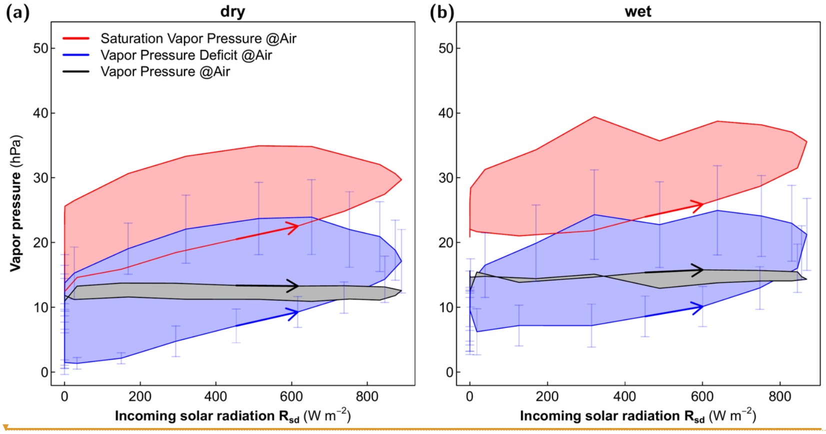

Figure 11: Diurnal patterns of vapor pressure in air (black), the saturated vapor pressure evaluated at observed air temperature (red), and the vapor pressure deficit (blue) for (a) dry and (b) wet days.

Deleted:

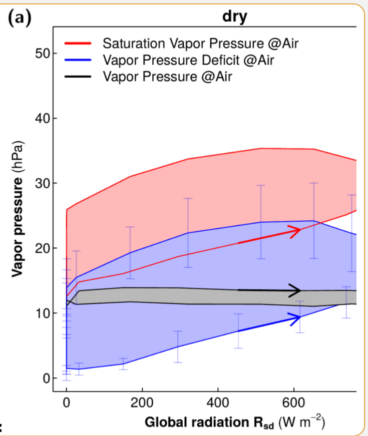

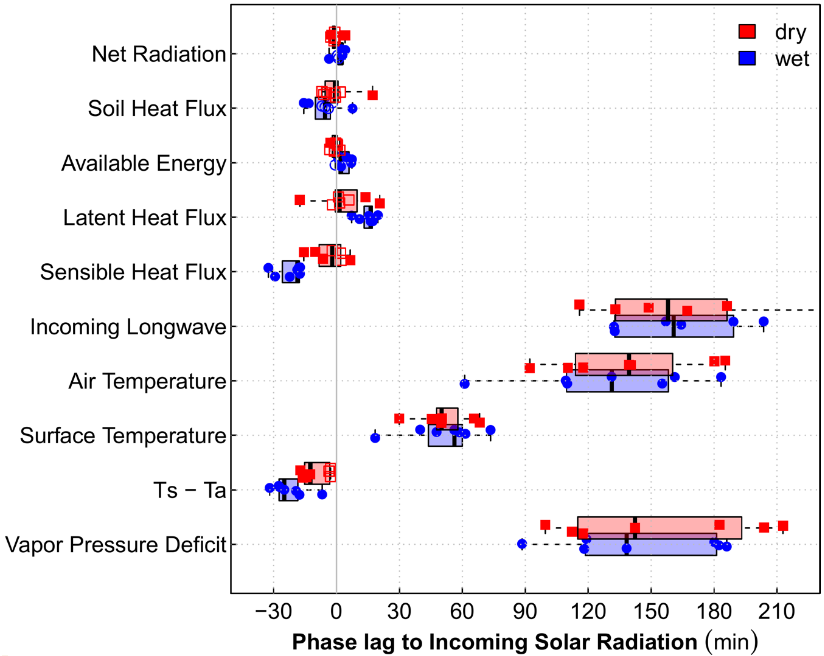

Figure 12: Phase lag to solar radiation of surface energy fluxes and surface state variables used as input for the evapotranspiration models for dry (red) and wet (blue) days. Boxplot and daily estimates with filled symbols showing significant phase lag estimates.

Deleted:

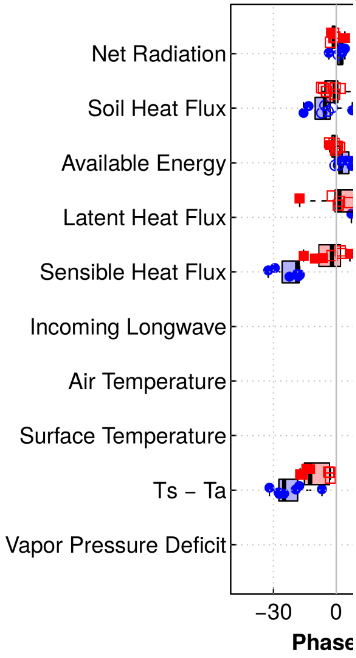

4 Discussion

4.1 Dominant controls of λE at the diurnal cycle

Our analysis of the diurnal cycle showed that λE follows the diurnal course of incoming solar radiation, explaining most of the variance in λE. However, a significant non-linearity in form of a phase lag between λE and R_{sd} was detected which showed larger λE for the same R_{sd} in the afternoon as in the morning. We found that the lag in λE is accompanied by a preceding phase lag of the sensible heat flux, while the other surface energy balance components (e.g., net radiation and soil heat flux) revealed very small phase lags with R_{sd}. Hence, there is compensation between the phase shifts of sensible and latent heat fluxes, which becomes more apparent under the wet conditions. Our results are consistent with comprehensive FLUXNET studies of Wilson et al. (2003) and Nelson et al. (2018) which used a different metric (median centroid) for assessing diurnal phase shifts. Wilson et al. (2003) found that H precedes λE at most sites, with the exception of sites in a Mediterranean climate. Using the FLUXNET2015 dataset, Nelson et al. (2018) found that the median centroid of λE occurs predominantly in the afternoon across all plant functional types when $f_E > 0.35$, while for very dry conditions ($f_E < 0.2$) a shift of the λE centroid towards the morning was found. This indicates that our results are not just applicable to Luxembourg, but are a general phenomenon which justifies a wider interpretation within temperate climates.

It is important to emphasize here, that the observed phase lags are not dominated by diurnal heat storage changes below the surface, since both the diurnal magnitude and the phase lag of the soil heat flux were relatively small compared to the turbulent heat fluxes. The models employed here use available energy (R_n–G) as input to estimate λE. However, the phase lag of the latent heat flux would only reduce by about 3 min when choosing R_n-G instead of R_{sd} as reference variable to calculate the phase lags. Hence, the observed phase lags of λE and H to R_{sd} are not an artifact of the analysis, but can be considered as an imprint of L-A interaction.

The obtained phase lags of the surface fluxes and variables allow for a process-based insight into the diurnal heat exchange of the surface with the atmosphere. Since there is only limited heat storage in the surface layer itself, which explains the small phase lags of the heat fluxes, the heating imbalance caused by solar radiation must be effectively redistributed. Over land it is the lower atmosphere which acts as efficient heat storage to buffer most of the diurnal imbalance caused by solar radiation, because the heat storage of the subsurface is limited by the relatively slow heat conduction into the soil. Thus, the lower atmosphere is effectively heated by surface longwave emission and the sensible heat flux, which in combination with the diurnal cycle of vertically transported turbulent kinetic energy (TKE) leads to the development of the convective planetary boundary layer (CBL) (e.g., Oke 1987). The changes in heat storage in the CBL are reflected by the very large phase lags for air temperature and longwave downwelling radiation, which both have a phase lag of about 2.5h. This large phase lag of air temperature then shapes (i) the vertical surface-air temperature gradient, which drives the sensible heat flux, and (ii) the vapor pressure deficit of the air. Despite the complexity of processes within the convective boundary layer, including the morning transition and entrainment at its top, we find that all surface energy components correlate strongly with solar radiation (Table 4). What this suggests is that the state of the surface-atmosphere system is predominantly shaped by fluxes, particularly by solar radiation as its primary driver, with the state in terms of temperatures and humidity gradients adjusting to these fluxes, rather than the reverse, where the state (in terms of temperature and humidity) drives the fluxes.

Deleted: While the soil heat flux

Deleted: , the lower atmosphere acts as efficient heat storage

We also found that the phase lag of the turbulent heat fluxes is affected by soil water availability. This is most clearly seen for the surface-air temperature gradient and the sensible heat flux, whose phase lag is two times larger for wet than for dry days. This means that for the same solar radiation forcing we find higher values of the sensible heat flux in the morning than in the afternoon. The effect of water availability is also seen for the phase lag of the latent heat flux and to a lesser extent for the soil heat flux.

Deleted: These interactions are

Deleted: , as reflected in the phase lags

Deleted: These

Our findings agree well with studies which use the diurnal centroid method, showing that moisture limitation decreases the lag in timing of λE (Wilson et al. 2003, Xiang et al., 2017, Nelson et al., 2018). The phase shift of D_a might enhance evaporation at the cost of the sensible heat flux during the afternoon under sufficient moisture availability. However, under drier conditions, our findings suggest that the surface heats more strongly and generates more buoyancy, which is reflected by higher aerodynamic conductances as compared to the wet conditions (Fig. 10). The larger aerodynamic conductance would then enable a more effective sensible heat exchange, and would thus lower the phase difference between the sensible and latent heat fluxes.

Note, that our interpretation disregards the effects of horizontal advection of moisture and temperature. Events of strong advection, e.g. of temperature can add heat to the surface energy balance and thus alter the diurnal cycle. Similarly, events of dry air advection may enhance local λE at the cost of the sensible heat flux. Since we used composite averages and statistics over a set of days we aim to reduce the impact of such advective events. We expect that it is unlikely that such events occurred throughout all wet / dry days in a consistent manner.

4.2 Using phase lags to identify model biases

Our comparison of different modeling approaches shows that by using phase lags, one can identify biases in evapotranspiration parameterizations and relate these towards processes for a better understanding of surface-atmosphere interactions under different conditions of water availability. One of our main findings is that the surface energy balance fluxes and the temperature gradient have a comparatively small phase lag to the incoming solar radiation, while air temperature and vapor pressure deficit have substantial phase lags. This difference in phase lags can then be used to infer biases in estimates of evapotranspiration. In our application of this approach to observations of one site in a temperate climate we found that evapotranspiration exhibits a comparatively small phase lag, indicating that it was dominantly driven by solar radiation and temperature gradients, and not by the water vapor pressure deficit. Our findings are in line with observations of a near linear relationship of λE to R_{sd} by Jackson et al., 1983 which stimulated remote sensing based spatial mapping of λE (Crago, 1996). Also the semi-empirical Makkink equation to estimate potential evapotranspiration (Makkink 1957, De Bruin and Lablans 1997, De Bruin et al., 2015) uses R_{sd} as main driver.

Deleted: air temperature and the water vapor pressure deficit. This

Further support of the argument is given by the successful application of equilibrium evapotranspiration (Schmidt 1915, Priestley-Taylor 1972, Miralles et al., 2011, Renner et al., 2016) which uses R_n and air temperature as key inputs.

Moved (insertion) [1]

Our interpretation is consistent with studies of non-water-stressed evapotranspiration that is best represented by potential evapotranspiration schemes which are primarily driven by net radiation, as demonstrated for FLUXNET observations by Maes et al., (2018) and for climate model simulations by Milly and Dunne, (2016). Milly and Dunne (2016) interpreted these findings in terms of strong feedbacks between the surface and the atmosphere, which couple the surface variables and which result in a top-down energy constraint that is well captured by energy-only formulations.

Our analysis allows to better understand the relevance of the feedbacks which occur at a sub-daily time scale. These feedbacks are driven by the redistribution of heat gained by absorption of solar radiation at the surface, which causes a significant co-variation of the input variables to incoming solar radiation (Table 4). This is especially important for the vapor pressure deficit of the air which acts as a driver of λE and is also known to affect the stomatal conductance (Jarvis 1976, Jarvis and McNaughton 1986). De Bruin and Holtslag (1982) showed that a positive correlation between D_a and R_n allows simplifying the complex PM equation to a form similar to equilibrium evaporation (Eq. 8) with net radiation as the dominant driver. Therefore, simpler, energy based formulations for λE show similar performance as PM based approaches, but with less input parameters (De Bruin and Holtslag 1982, Beljaars and Bosveld 1997). The challenge of the PM equation is then a parameterization of the conductances, which must capture the feedbacks included in the input data. Since the co-variation originates from the diurnal redistribution of heat, a mismatch would then clearly be seen at the sub-daily timescale. Hence by focusing on the internal relationship of the modeled λE to R_{sd} at the sub-daily time scale we found that (i) the Penman-Monteith based approaches showed a consistently larger phase lag than what was actually observed and (ii) these approaches did not show a reduction of the phase lag under dry conditions. The PM approaches use the vapor pressure deficit as an input which showed a substantial hysteresis loop in the order of 2.5 h lagging R_{sd}. This is due to the temperature dependency of the saturation vapor pressure, while the actual vapor pressure shows no relationship with R_{sd}. Besides D_a, all other input variables to the Penman-Monteith approaches used here (both FAO and STIC) showed minor phase lags with respect to R_{sd}. Since the surface conductance in FAO Penman-Monteith is fixed with time, the resulting prediction of potential λE showed a significant and large phase lag in the order of 0.5 h. Even when we use the observed aerodynamic conductance as input, the effect remains the same, which emphasizes that a constant surface conductance results in biases in the diurnal cycle of λE. In contrast to assuming a constant g_s, STIC computes λE through analytical estimation of g_s and g_{av} from the information of both, the surface-air temperature gradient and the vapor pressure deficit. This dynamic treatment of g_s reduced the phase lag to values similar as the observations under the wet conditions. However, under dry conditions STIC still showed significant phase lags, which may be related to the lag of D_a to R_{sd} which was similar for both dry and wet conditions (Fig. 12). Hence, our analysis indicates that the PM-based approaches used here overestimated the effect of water vapor deficit on actual evapotranspiration, which, in the end, reflects in the estimation of the surface and the aerodynamic conductance to water vapor.

Deleted: 7

Deleted: diurnal

Deleted: diurnal

Deleted: variable

Deleted: Given that

Deleted: 12), λE from STIC also revealed a similar pattern and there was no substantial difference in phase lag of λE from STIC between the wet and dry conditions.

The temperature-gradient approaches used here (OSEB and TSEB) are structurally different from the PM approaches, since they infer λE from the residual of the surface energy balance and thus do not explicitly deal with the aerodynamic and surface conductance of water vapor. The phase lag analysis of the environmental variables used to drive the predictive models of λE helped to identify an important benefit of the temperature-gradient approaches over the Penman-Monteith based approach.
The temperature-gradient approaches employ the vertical temperature gradient (T_s - T_a) which showed a significant counter-clockwise, i.e. a leading hysteretic loop, which is in the order of the phase shift detected for the sensible heat flux (Fig. 12). In addition, there is a distinct and significant increase of the phase shift in both the temperature gradient and the sensible heat flux under the wet conditions. Hence,

the temperature gradient as input contains valuable information on water limitation in terms of the magnitude (i.e. the slope of ($T_s - T_a$) to R_{sd}) and the diurnal phase lag (see Table 4).

While the PM approaches must identify two conductances simultaneously, the temperature-gradient approaches only need to parameterize the aerodynamic conductance to heat (g_{ah}) using wind-speed as input. Thereby we found that these approaches agreed well with the approximated g_{ah} from the EC tower, which shows an enhanced conductance under dry conditions. Contrarily, the diagnosed g_{av} from STIC did not show substantial differences between dry and wet conditions, pointing to the difficulty of the analytical approach and its associated assumptions to identify two bulk conductances parameters from the available radiometric and meteorological data (Mallick et al., 2018) for the climatic conditions in which these were evaluated here.

Note, that we evaluated a temperate grassland site which experienced an exceptional summer drought. Thereby, the evaporative fraction did not decline below 0.3. In semi-arid ecosystems the evaporative fraction may decrease substantially below 0.3 and Nelson et al., 2018 showed that there is a morning shift of λE (analogous to a negative phase lag) under very dry conditions ($f_{\mathrm{E}} < 0.2$). This points towards a different stomatal regulation changing the diurnal course of surface conductance. While it was shown by Bhattarai et al., (2018) that STIC performs well also under semi-arid conditions, temperature-gradient approaches can show larger biases under semi-arid conditions (Morillas et al., 2013). The difficulty of temperature-gradient approaches are predominantly in the parameterization of aerodynamic conductance of heat which becomes more challenging under these very dry conditions (Kustas et al., 2016).

The relevance of the diurnal time scale for the problem of surface conductance parameterizations was already highlighted by Matheny et al., 2014. However, they and others evaluated the diurnal patterns of the hysteretic loops between λE and D_{a} (see also Zhang et al., 2014, Zheng et al., 2014). Given that solar radiation is the cause of the strong L-A feedbacks at the diurnal time scale we believe that solar radiation is better suited as a reference variable than D_{a}. Our results show that the new metric of the phase lag of heat fluxes and surface states to incoming solar radiation reveals important biases of evapotranspiration schemes. These biases may well be compensated for at a longer time scales (Matheny et al., 2014) but would lead to biased sensitivities with respect to climate change (Milly and Dunne 2016). Here, we applied the phase lag metric to observationally driven evapotranspiration schemes. In the future, we plan to apply these new metrics based on hysteretic loops to model outputs of land-surface models (such as NOAH-MP, Niu et al., 2011) as well as of fully coupled surface-atmosphere simulations in order to detect and to identify errors in the parameterization of state-of-the-art LSMs.

5 Conclusions

We analyzed the relationship of surface heat fluxes and states to incoming solar radiation at the sub-daily timescale for a temperate grassland site which experienced a summer drought. Most variables

Deleted: often used in remote sensing.

Deleted: quantified

Deleted: non-linear

Deleted: evapotranspiration

Deleted: in terms of a phase lag

Deleted: diurnal time scale. Our findings have practical implications for remote sensing based λE retrievals and for land-surface model evaluation and calibration. We evaluated three structurally different schemes which are used in remote sensing based applications

Deleted: grass

Deleted: Our results

showed significant hysteresis loops which we objectively quantified by a linear component and a non-linear phase lag component using multiple linear regression and harmonic analysis. We then compared these diurnal signatures obtained from observations of an Eddy-Covariance station with commonly used but structurally different approaches to model actual and potential evapotranspiration. The models have been forced by the observational data such that the differences to observations can be attributed to model formulation and signals contained in the input data. Our analysis guides model selection with a preference for the temperature gradient approaches, because the vertical temperature gradient contains relevant signals of soil moisture limitation as opposed to the vapor pressure deficit of the air. Furthermore, schemes which use vapor pressure deficit as additional input (such as the Penman-Monteith formulation), require a dynamic, i.e. time dependent characterization of surface conductance to account for the strong phase lag in vapor pressure deficit. Hence, our results suggest that simpler λE approaches based on the surface energy balance and surface temperature may be more suitable to estimate evapotranspiration from observational data (e.g. remote sensing data) in climates without substantial water stress. Apparently, the surface observations already contain the imprint of land-atmosphere interactions, whereas in the case of coupled land surface-atmosphere models these interactions are explicitly resolved. Hence, detailed models of aerodynamic and surface conductance and its interaction with the environment are of crucial importance for skillful climate predictions including the carbon cycle (Prentice et al., 2014, Wolf et al., 2016; Konings et al., 2017).

We suggest that an evaluation of these schemes should be based on the sub-daily time scale, because a land-atmosphere exchange scheme must accomplish a balance between the surface energy balance with small imprints of heat storage changes and the lower atmosphere with strong imprints of heat storage changes (Kleidon and Renner 2017). Although a mismatch of the diurnal patterns may not be detected at the aggregated time scales of days and months, it may lead to biased model sensitivities (Matheny et al., 2014). For example, an overly sensitive formulation of evapotranspiration to vapor pressure deficit and thus to temperature would predict larger changes in potential evapotranspiration under global warming (Milly and Dunne 2016). Here, we analyzed observationally driven evapotranspiration schemes and their inputs, which revealed an apparent energy constraint. This constraint, which appears as strong correlation of surface fluxes and gradients to incoming solar radiation should be correctly represented by any land-surface model which resolves the land-atmosphere interaction. While this may sound trivial, recent benchmarking studies showed that current state-of-the-art land-surface models have difficulties to represent the strong link of turbulent heat fluxes to solar radiation (Best et al., 2015; Haughton et al., 2016). Our findings provide an explanation of this model deficiency and we suggest that further information is gained by evaluating land surface schemes in terms of phase lags in surface fluxes and states such as the sensible and soil heat flux including the diurnal dynamics of surface and air temperatures. Correctly representing these metrics will lead towards a more accurate representation of the diurnal heat and mass exchange of the land with the atmosphere.

Deleted: that

Deleted: schemes show a higher correlation and thus better represent the diurnal cycle than a combined

Deleted: -vapor

Deleted: scheme. What this means is that for our site, the temperature gradient between the surface and the near-surface atmosphere contained more important information

Deleted: water

Deleted: than

Deleted: water

Deleted: (which is also difficult to retrieve from remote sensing (Kalma et al., 2008, Yang et al., 2015)).

Deleted: It would seem that these

Deleted: diurnal

Deleted: seen

Deleted:) which

Deleted: be crucial for assessing climate change impacts

Deleted: why

Deleted: is so difficult to achieve

Deleted: temperature

6 Code availability

The data analysis was performed with the open-source environment R (www.r-project.org). Functions to calculate the phase lag are provided as R-package “phaselag” available from github at https://github.com/laubblatt/phaselag . The script to perform data analysis and figures can be obtained from https://github.com/laubblatt/2018_DiurnalEvaporation. Code to perform OSEB and TSEB simulations can be found at https://github.com/ClaireBrenner/pyTSEB_Renner_et_al_2018. Code to simulate STIC1.2 simulations is available upon request at Kaniska Mallick (LIST, kaniska.mallick@list.lu).

Commented [MR2]: Update when R code published in github and zenodo

Commented [MR3]: @Claire can we put this on zenodo as well?

Deleted: Code to perform data analysis and figures can be obtained from the main author upon request.

7 Data availability

Data of observations and model output used in this study can be obtained from the research data repository GFZ Data Services http://dataservices.gfz-potsdam.de. Observational data (Wizemann et. al., 2018): http://pmd.gfz-potsdam.de/panmetaworks/review/24caec4ac751a29e7049035dd5a1a2c4f12ea1670772794987684f34abeddafc/ . Model output data (Renner et. al.,): http://pmd.gfz-potsdam.de/panmetaworks/review/7a6982ed557e3a9844fa7f0d3cde4f4cd8fccdbbb93a3e838a57ca08ab8b4cac

Deleted: Data can be obtained upon request from the main author. Observational data from the EC site can be obtained from Hans-Dieter Wizemann, hans-dieter.wizemann@uni-hohenheim.de.

Commented [MR4]: Update when review process at GFZ finished

Wizemann, Hans-Dieter; Trebs, Ivonne; Wulfmeyer, Volker (2018): Surface energy balance observations at a grassland site in Luxembourg. GFZ Data Services. http://doi.org/10.5880/fidgeo.2018.024

Renner, Maik; Wizemann, Hans-Dieter; Brenner, Claire; Mallick, Kaniska; Trebs, Ivonne; Wulfmeyer, Volker; Schulz, Karsten; Kleidon, Axel (2018): Surface energy balance at a grassland site in Luxembourg modelled by three structurally different evapotranspiration schemes. GFZ Data Services. http://doi.org/10.5880/fidgeo.2018.019

8 Author contribution

MR and AK conceived the analysis of the diurnal cycle. VW, KS and IT designed the field campaign. HW carried out the EC measurements and EC data processing. CB performed OSEB/TSEB simulations. KM performed STIC1.2 simulations. MR merged the data and performed data analysis. MR and LC developed the phase lag computation. JW provided ancillary simulation data. IT provided climate information. MR prepared the manuscript with contributions from all co-authors.

9 Competing interests

The authors declare that they have no conflict of interest.

10 Special issue statement

This draft shall contribute to the upcoming Joint special issue in HESS (lead journal) and ESSD: Linking landscape organisation and hydrological functioning: from hypotheses and observations to concepts, models and understanding

11 Acknowledgements

This study was supported by the German Research Foundation (DFG) through funding of the research unit "From Catchments as Organised Systems to Models based on Dynamic Functional Units – CAOS" (FOR 1598) within the sub-project "Understanding and characterizing land surface-atmosphere exchange and feedbacks" (Project number 182331427). MR and KL were funded by DFG grant number (KL 2168/2-1). CB was supported by the Austrian Science Fund (FWF) through funding of the CAOS Research Unit (I 2142-N29). KM was supported by the Luxembourg Institute of Science and Technology (LIST) through the project BIOTRANS (grant number 00001145), CAOS-2 project grant (INTER/DFG/14/02) funded by FNR (Fonds National de la Recherche)–DFG, and HiWET consortium funded by the Belgian Science Policy (BELSPO) – FNR under the programme STEREOIII (INTER/STEREOIII/13/03/HiWET; CONTRACT NR SR/00/301).
IT was supported by the Luxembourg Institute of Science and Technology (LIST) through the project BIOTRANS (grant number 00001145).

12 References

Alduchov, O. A. and Eskridge, R. E.: Improved Magnus Form Approximation of Saturation Vapor Pressure, J. Appl. Meteor., 35(4), 601–609, doi:10.1175/1520-0450(1996)035<0601:IMFAOS>2.0.CO;2, 1996.
Alfieri, J. G., Anderson, M. C., Kustas, W. P. and Cammalleri, C.: Effect of the revisit interval and temporal upscaling methods on the accuracy of remotely sensed evapotranspiration estimates, Hydrol. Earth Syst. Sci., 21(1), 83–98, doi:10.5194/hess-21-83-2017, 2017.
Allen, R. G., Pereira, L. S., Raes, D. and Smith, M.: Crop evapotranspiration-Guidelines for computing crop water requirements-FAO Irrigation and drainage paper 56, FAO, Rome, 300, 6541, 1998.
Anderson, M. C., Norman John M., Mecikalski John R., Otkin Jason A. and Kustas William P.: A climatological study of evapotranspiration and moisture stress across the continental United States based on thermal remote sensing: 1. Model formulation, Journal of Geophysical Research: Atmospheres, 112(D10), doi:10.1029/2006JD007506, 2007.
Anon:, n.d.
Beljaars, A. C. M. and Bosveld, F. C.: Cabauw Data for the Validation of Land Surface Parameterization Schemes, J. Climate, 10(6), 1172–1193, doi:10.1175/1520-0442(1997)010<1172:CDFTVO>2.0.CO;2, 1997.

Moved (insertion) [2]

Deleted: :10.1029/2006JD007506,

Deleted: :10.1175/1520-0442(1997)010<1172:CDFTVO>2.0.CO;2,

Best, M. J., Abramowitz, G., Johnson, H. R., Pitman, A. J., Balsamo, G., Boone, A., Cuntz, M., Decharme, B., Dirmeyer, P. A., Dong, J., Ek, M., Guo, Z., Haverd, V., van den Hurk, B. J. J., Nearing, G. S., Pak, B., Peters-Lidard, C., Santanello, J. A., Stevens, L. and Vuichard, N.: The Plumbing of Land Surface Models: Benchmarking Model Performance, Journal of Hydrometeorology, 16(3), 1425–1442, doi:10.1175/JHM-D-14-0158.1, 2015.

Betts, A. K.: FIFE atmospheric boundary layer budget methods, Journal of Geophysical Research: Atmospheres, 97(D17), 18523–18531, 1992.

Beven, K.: A sensitivity analysis of the Penman-Monteith actual evapotranspiration estimates, Journal of Hydrology, 44(3–4), 169–190, doi:10.1016/0022-1694(79)90130-6, 1979.

Bhattarai, N., Mallick, K., Brunsell, N. A., Sun, G. and Jain, M.: Regional evapotranspiration from an image-based implementation of the Surface Temperature Initiated Closure (STIC1.2) model and its validation across an aridity gradient in the conterminous US, Hydrol. Earth Syst. Sci., 22(4), 2311–2341, doi:10.5194/hess-22-2311-2018, 2018.

Brenner, C., Thiem, C. E., Wizemann, H.-D., Bernhardt, M. and Schulz, K.: Estimating spatially distributed turbulent heat fluxes from high-resolution thermal imagery acquired with a UAV system, International Journal of Remote Sensing, 38(8–10), 3003–3026, doi:10.1080/01431161.2017.1280202, 2017.

de Bruin, H. a. R. and Lablans, W. N.: Reference crop evapotranspiration determined with a modified Makkink equation, Hydrol. Process., 12(7), 1053–1062, doi:10.1002/(SICI)1099-1085(19980615)12:7<1053::AID-HYP639>3.0.CO;2-E, 1998.

de Bruin, H. a. R., Trigo, I. F., Bosveld, F. C. and Meirink, J. F.: A Thermodynamically Based Model for Actual Evapotranspiration of an Extensive Grass Field Close to FAO Reference, Suitable for Remote Sensing Application, J. Hydrometeor, 17(5), 1373–1382, doi:10.1175/JHM-D-15-0006.1, 2015.

Brutsaert, W.: Hydrology: an introduction, Wiley Online Library., 2005.

Brutsaert, W. and Stricker, H.: An Advection-Aridity Approach to Estimate Actual Regional Evapotranspiration, Water Resources Research, 15(2), 1979.

Camuffo, D. and Bernardi, A.: An observational study of heat fluxes and their relationships with net radiation, Boundary-Layer Meteorol, 23(3), 359–368, doi:10.1007/BF00121121, 1982.

Choi, M., Kustas, W. P., Anderson, M. C., Allen, R. G., Li, F. and Kjaersgaard, J. H.: An intercomparison of three remote sensing-based surface energy balance algorithms over a corn and soybean production region (Iowa, US) during SMACEX, Agricultural and Forest Meteorology, 149(12), 2082–2097, 2009.

Crago, R. and Brutsaert, W.: Daytime evaporation and the self-preservation of the evaporative fraction and the Bowen ratio, Journal of Hydrology, 178(1), 241–255, doi:10.1016/0022-1694(95)02803-X, 1996.

Crago, R. D.: Conservation and variability of the evaporative fraction during the daytime, Journal of Hydrology, 180(1), 173–194, doi:10.1016/0022-1694(95)02903-6, 1996.

De Bruin, H. a. R. and Holtslag, A. a. M.: A Simple Parameterization of the Surface Fluxes of Sensible and Latent Heat During Daytime Compared with the Penman-Monteith Concept, J. Appl. Meteor., 21(11), 1610–1621, doi:10.1175/1520-0450(1982)021<1610:ASPOTS>2.0.CO;2, 1982.

Deleted: :10.1175/JHM-D-14-0158.1,

Deleted: :10.1016/0022-1694(79)90130-6,

Deleted: :10.5194/hess-22-2311-2018,

Deleted: :10.1080/01431161.2017.1280202,

Deleted: :10.1002/(SICI)1099-1085(19980615)12:7<1053::AID-HYP639>3.0.CO;2-E,

Deleted: :10.1175/JHM-D-15-0006.1,

Deleted: :10.1007/BF00121121,

Deleted: :10.1016/0022-1694(95)02903-6,

Deleted: :10.1175/1520-0450(1982)021<1610:ASPOTS>2.0.CO;2,

Duan, Z. and Bastiaanssen, W. G. M.: Evaluation of three energy balance-based evaporation models for estimating monthly evaporation for five lakes using derived heat storage changes from a hysteresis model, Environ. Res. Lett., 12(2), 024005, doi:10.1088/1748-9326/aa568e, 2017.

Duchon, C. and Hale, R.: Time series analysis in meteorology and climatology: an introduction, John Wiley & Sons., 2012.

Foken, T.: The energy balance closure problem: An overview, Ecological Applications, 18(6), 1351–1367, doi:10.1890/06-0922.1, 2008.

French, A. N., Hunsaker, D. J. and Thorp, K. R.: Remote sensing of evapotranspiration over cotton using the TSEB and METRIC energy balance models, Remote Sensing of Environment, 158, 281–294, 2015.

Fuchs, M. and Hadas, A.: The heat flux density in a non-homogeneous bare loessial soil, Boundary-Layer Meteorol, 3(2), 191–200, doi:10.1007/BF02033918, 1972.

Haughton, N., Abramowitz, G., Pitman, A. J., Or, D., Best, M. J., Johnson, H. R., Balsamo, G., Boone, A., Cuntz, M., Decharme, B., Dirmeyer, P. A., Dong, J., Ek, M., Guo, Z., Haverd, V., van den Hurk, B. J. J., Nearing, G. S., Pak, B., Santanello, J. A., Stevens, L. E. and Vuichard, N.: The Plumbing of Land Surface Models: Is Poor Performance a Result of Methodology or Data Quality?, J. Hydrometeor., 17(6), 1705–1723, doi:10.1175/JHM-D-15-0171.1, 2016.

van Heerwaarden, C. C., Vilà-Guerau de Arellano, J., Gounou, A., Guichard, F. and Couvreux, F.: Understanding the Daily Cycle of Evapotranspiration: A Method to Quantify the Influence of Forcings and Feedbacks, Journal of Hydrometeorology, 11(6), 1405–1422, doi:10.1175/2010JHM1272.1, 2010.

Ingwersen, J., Steffens, K., Högy, P., Warrach-Sagi, K., Zhunusbayeva, D., Poltoradnev, M., Gäbler, R., Wizemann, H.-D., Fangmeier, A., Wulfmeyer, V. and Streck, T.: Comparison of Noah simulations with eddy covariance and soil water measurements at a winter wheat stand, Agricultural and Forest Meteorology, 151(3), 345–355, doi:10.1016/j.agrformet.2010.11.010, 2011.

Jackson, R. D., Hatfield, J. L., Reginato, R. J., Idso, S. B. and Pinter, P. J.: Estimation of daily evapotranspiration from one time-of-day measurements, Agricultural Water Management, 7(1–3), 351–362, 1983.

Jarvis, P. G.: The interpretation of the variations in leaf water potential and stomatal conductance found in canopies in the field, Phil. Trans. R. Soc. Lond. B, 273(927), 593–610, doi:10.1098/rstb.1976.0035, 1976.

Jarvis, P. G. and McNaughton, K. G.: Stomatal control of transpiration: scaling up from leaf to region, in Advances in ecological research, vol. 15, pp. 1–49, Elsevier., 1986.

Jiménez, P. A., Dudhia, J., González-Rouco, J. F., Navarro, J., Montávez, J. P. and García-Bustamante, E.: A revised scheme for the WRF surface layer formulation, Monthly Weather Review, 140(3), 898–918, 2012.

Jury, W. A. and Horton, R.: Soil Physics, 6th ed., John Wiley & Sons, Inc., 2004.

Kalma, J. D., McVicar, T. R. and McCabe, M. F.: Estimating Land Surface Evaporation: A Review of Methods Using Remotely Sensed Surface Temperature Data, Surv Geophys, 29(4–5), 421–469, doi:10.1007/s10712-008-9037-z, 2008.

Kleidon, A. and Renner, M.: Thermodynamic limits of hydrologic cycling within the Earth system: concepts, estimates and implications, Hydrol. Earth Syst. Sci., 17(7), 2873–2892, doi:10.5194/hess-17-2873-2013, 2013.

Deleted: :10.1088/1748-9326/aa568e,

Deleted: :10.1890/06-0922.1,

Deleted: :10.1007/BF02033918,

Deleted: :10.1175/JHM-D-15-0171.1,

Deleted: :10.1016/j.agrformet.2010.11.010,

Deleted: :10.1098/rstb.1976.0035,

Deleted: :10.1007/s10712-008-9037-z,

Deleted: :10.5194/hess-17-2873-2013,

Kleidon, A. and Renner, M.: An explanation for the different climate sensitivities of land and ocean surfaces based on the diurnal cycle, Earth Syst. Dynam., 8(3), 849–864, doi:10.5194/esd-8-849-2017, 2017.

Konings, A. G., Williams, A. P. and Gentine, P.: Sensitivity of grassland productivity to aridity controlled by stomatal and xylem regulation, Nature Geoscience, 10(4), 284–288, doi:10.1038/ngeo2903, 2017.

Kustas, W. P. and Norman, J. M.: Evaluation of soil and vegetation heat flux predictions using a simple two-source model with radiometric temperatures for partial canopy cover, Agricultural and Forest Meteorology, 94(1), 13–29, doi:10.1016/S0168-1923(99)00005-2, 1999.

Kustas, W. P., Nieto, H., Morillas, L., Anderson, M. C., Alfieri, J. G., Hipps, L. E., Villagarcía, L., Domingo, F. and Garcia, M.: Revisiting the paper "Using radiometric surface temperature for surface energy flux estimation in Mediterranean drylands from a two-source perspective," Remote Sensing of Environment, 184, 645–653, doi:10.1016/j.rse.2016.07.024, 2016.

Maes, W. H., Gentine, P., Verhoest, N. E. C. and Miralles, D. G.: Potential evaporation at eddy-covariance sites across the globe, Hydrology and Earth System Sciences Discussions, 1–38, doi:https://doi.org/10.5194/hess-2018-470, 2018.

Magnus, G.: Versuche über die Spannkräfte des Wasserdampfs, Ann. Phys., 137(2), 225–247, doi:10.1002/andp.18441370202, 1844.

Makkink, G.: Testing the Penman formula by means of lysimeters, J. Inst. Water Eng, 11(3), 277–288, 1957.

Mallick, K., Jarvis, A. J., Boegh, E., Fisher, J. B., Drewry, D. T., Tu, K. P., Hook, S. J., Hulley, G., Ardö, J., Beringer, J., Arain, A. and Niyogi, D.: A Surface Temperature Initiated Closure (STIC) for surface energy balance fluxes, Remote Sensing of Environment, 141, 243–261, doi:10.1016/j.rse.2013.10.022, 2014.

Mallick, K., Boegh, E., Trebs, I., Alfieri, J. G., Kustas, W. P., Prueger, J. H., Niyogi, D., Das, N., Drewry, D. T., Hoffmann, L. and Jarvis, A. J.: Reintroducing radiometric surface temperature into the Penman-Monteith formulation, Water Resour. Res., 51(8), 6214–6243, doi:10.1002/2014WR016106, 2015.

Mallick, K., Trebs, I., Boegh, E., Giustarini, L., Schlerf, M., Drewry, D. T., Hoffmann, L., von Randow, C., Kruijt, B., Araùjo, A., Saleska, S., Ehleringer, J. R., Domingues, T. F., Ometto, J. P. H. B., Nobre, A. D., de Moraes, O. L. L., Hayek, M., Munger, J. W. and Wofsy, S. C.: Canopy-scale biophysical controls of transpiration and evaporation in the Amazon Basin, Hydrol. Earth Syst. Sci., 20(10), 4237–4264, doi:10.5194/hess-20-4237-2016, 2016.

Mallick, K., Toivonen, E., Trebs, I., Boegh, E., Cleverly, J., Eamus, D., Koivusalo, H., Drewry, D., Arndt, S. K., Griebel, A., Beringer, J. and Garcia, M.: Bridging Thermal Infrared Sensing and Physically-Based Evapotranspiration Modeling: From Theoretical Implementation to Validation Across an Aridity Gradient in Australian Ecosystems, Water Resources Research, 54, doi:10.1029/2017WR021357, 2018.

Massman, W. J.: Correcting errors associated with soil heat flux measurements and estimating soil thermal properties from soil temperature and heat flux plate data, Agricultural and Forest Meteorology, 59(3), 249–266, doi:10.1016/0168-1923(92)90096-M, 1992.

Deleted: :10.5194/esd-8-849-2017,

Deleted: Knauer, J., Zaehle, S., Medlyn, B. E., Reichstein, M., Williams, C. A., Migliavacca, M., De Kauwe, M. G., Werner, C., Keitel, C. and Kolari, P.: Towards physiologically meaningful water-use efficiency estimates from eddy covariance data, Global change biology, 24(2), 694–710, 2018.¶

Deleted: :10.1038/ngeo2903,

Deleted: :10.1016/S0168-1923(99)00005-2,

Deleted: :10.1016/j.rse.2016.07.024,

Deleted: Hydrol.

Moved up [2]: Earth Syst. Sci

Deleted: . Discuss., 2018, 1–33, doi:10.5194/hess-2017-682,

Deleted: :10.1002/andp.18441370202,

Deleted: :10.1016/j.rse.2013.10.022,

Deleted: :10.1002/2014WR016106,

Deleted: :10.5194/hess-20-4237-2016,

Deleted: :10.1029/2017WR021357,

Deleted: :10.1016/0168-1923(92)90096-M,

Matheny, A. M., Bohrer, G., Stoy, P. C., Baker, I. T., Black, A. T., Desai, A. R., Dietze, M. C., Gough, C. M., Ivanov, V. Y., Jassal, R. S., Novick, K. A., Schäfer, K. V. R. and Verbeeck, H.: Characterizing the diurnal patterns of errors in the prediction of evapotranspiration by several land-surface models: An NACP analysis, J. Geophys. Res. Biogeosci., 119(7), 2014JG002623, doi:10.1002/2014JG002623, 2014.

Mauder, M. and Foken, T.: Eddy-Covariance Software TK3, University of Bayreuth., 2015.

Milly, P. C. D. and Dunne, K. A.: Potential evapotranspiration and continental drying, Nature Climate Change, 6(10), 946–949, doi:10.1038/nclimate3046, 2016.

Miralles, D. G., Holmes, T. R. H., De Jeu, R. A. M., Gash, J. H., Meesters, A. G. C. A. and Dolman, A. J.: Global land-surface evaporation estimated from satellite-based observations, Hydrol. Earth Syst. Sci., 15(2), 453–469, doi:10.5194/hess-15-453-2011, 2011.

Monteith, J. L.: Evaporation and environment., SYMP SOC EXP BIOL, 19, 205–34, 1965.

Nelson, J. A., Carvalhais, N., Migliavacca, M., Reichstein, M. and Jung, M.: Water-stress-induced breakdown of carbon–water relations: indicators from diurnal FLUXNET patterns, Biogeosciences, 15(8), 2433–2447, doi:10.5194/bg-15-2433-2018, 2018.

Niu, G.-Y., Yang, Z.-L., Mitchell, K. E., Chen, F., Ek, M. B., Barlage, M., Kumar, A., Manning, K., Niyogi, D., Rosero, E., Tewari, M. and Xia, Y.: The community Noah land surface model with multiparameterization options (Noah-MP): 1. Model description and evaluation with local-scale measurements, Journal of Geophysical Research, 116(D12), doi:10.1029/2010JD015139, 2011.

Ohmura, A.: The development and the present status of energy balance climatology, Journal of the Meteorological Society of Japan. Ser. II, 92(4), 245–285, 2014.

Oke, T. R.: Boundary layer climates, Routledge, Londan and New York., 1987.

Penman, H. L.: Natural evaporation from open water, bare soil and grass, Proceedings of the Royal Society of London. Series A. Mathematical and Physical Sciences, 193(1032), 120, 1948.

Prentice, I. C., Dong, N., Gleason, S. M., Maire, V. and Wright, I. J.: Balancing the costs of carbon gain and water transport: testing a new theoretical framework for plant functional ecology, Ecology Letters, 17(1), 82–91, doi:10.1111/ele.12211, 2014.

Priestley, C. and Taylor, R.: On the assessment of surface heat flux and evaporation using large-scale parameters, Monthly weather review, 100(2), 81–92, 1972.

Renner, M., Hassler, S. K., Blume, T., Weiler, M., Hildebrandt, A., Guderle, M., Schymanski, S. J. and Kleidon, A.: Dominant controls of transpiration along a hillslope transect inferred from ecohydrological measurements and thermodynamic limits, Hydrology and Earth System Sciences, 20(5), 2063–2083, doi:10.5194/hess-20-2063-2016, 2016.

Renner, M., Wizemann, H.-D., Brenner, C., Mallick, K., Trebs, I., Wulfmeyer, V., Schulz, K. and Kleidon, A.: Surface energy balance observations and model output at a grassland site in Luxembourg, GFZ Data Services, doi:http://doi.org/10.5880/fidgeo.2018.019, 2018.

Santanello, J. A. and Friedl, M. A.: Diurnal Covariation in Soil Heat Flux and Net Radiation, J. Appl. Meteor., 42(6), 851–862, doi:10.1175/1520-0450(2003)042<0851:DCISHF>2.0.CO;2, 2003.

Santanello, J. A., Peters-Lidard, C. D., Kumar, S. V., Alonge, C. and Tao, W.-K.: A Modeling and Observational Framework for Diagnosing Local Land–Atmosphere Coupling on Diurnal Time Scales, J. Hydrometeor., 10(3), 577–599, doi:10.1175/2009JHM1066.1, 2009.

Deleted: :10.1002/2014JG002623,

Deleted: :10.1038/nclimate3046,

Deleted: :10.5194/hess-15-453-2011,

Deleted: :10.5194/bg-15-2433-2018,

Deleted: :10.1029/2010JD015139,

Deleted: :10.1111/ele.12211,

Deleted: :10.5194/hess-20-2063-2016,

Deleted: :10.1175/1520-0450(2003)042<0851:DCISHF>2.0.CO;2,

Deleted: :10.1175/2009JHM1066.1,

Santanello, J. A., Dirmeyer, P. A., Ferguson, C. R., Findell, K. L., Tawfik, A. B., Berg, A., Ek, M., Gentine, P., Guillod, B. P., van Heerwaarden, C., Roundy, J. and Wulfmeyer, V.: Land-Atmosphere Interactions: The LoCo Perspective, Bull. Amer. Meteor. Soc., doi:10.1175/BAMS-D-17-0001.1, 2017.

Schmidt, W.: Strahlung und Verdunstung an freien Wasserflächen; ein Beitrag zum Wärmehaushalt des Weltmeers und zum Wasserhaushalt der Erde, Ann. Calender Hydrographie und Maritimen Meteorologie, 43, 111–124, 1915.

Stoy, P. C., Mauder, M., Foken, T., Marcolla, B., Boegh, E., Ibrom, A., Arain, M. A., Arneth, A., Aurela, M., Bernhofer, C., Cescatti, A., Dellwik, E., Duce, P., Gianelle, D., van Gorsel, E., Kiely, G., Knohl, A., Margolis, H., McCaughey, H., Merbold, L., Montagnani, L., Papale, D., Reichstein, M., Saunders, M., Serrano-Ortiz, P., Sottocornola, M., Spano, D., Vaccari, F. and Varlagin, A.: A data-driven analysis of energy balance closure across FLUXNET research sites: The role of landscape scale heterogeneity, Agricultural and Forest Meteorology, 171–172, 137–152, doi:10.1016/j.agrformet.2012.11.004, 2013.

Stull, R. B.: An introduction to boundary layer meteorology, Kluwer Academic Publishers, Dordrecht, The Netherlands., 1988.

Tang, R., Li, Z.-L., Jia, Y., Li, C., Chen, K.-S., Sun, X. and Lou, J.: Evaluating one- and two-source energy balance models in estimating surface evapotranspiration from Landsat-derived surface temperature and field measurements, International Journal of Remote Sensing, 34(9–10), 3299–3313, doi:10.1080/01431161.2012.716529, 2013.

Thom, A. S.: Momentum, mass and heat exchange of vegetation, Q.J.R. Meteorol. Soc., 98(415), 124–134, doi:10.1002/qj.49709841510, 1972.

Timmermans, W. J., Kustas, W. P., Anderson, M. C. and French, A. N.: An intercomparison of the Surface Energy Balance Algorithm for Land (SEBAL) and the Two-Source Energy Balance (TSEB) modeling schemes, Remote Sensing of Environment, 108(4), 369–384, doi:10.1016/j.rse.2006.11.028, 2007.

Twine, T. E., Kustas, W. P., Norman, J. M., Cook, D. R., Houser, Pr., Meyers, T. P., Prueger, J. H., Starks, P. J. and Wesely, M. L.: Correcting eddy-covariance flux underestimates over a grassland, Agricultural and Forest Meteorology, 103(3), 279–300, 2000.

Wilson, K. B., Baldocchi, D., Falge, E., Aubinet, M., Berbigier, P., Bernhofer, C., Dolman, H., Field, C., Goldstein, A. and Granier, A.: Diurnal centroid of ecosystem energy and carbon fluxes at FLUXNET sites, Journal of Geophysical Research: Atmospheres, 108(D21), 2003.

Wizemann, H.-D., Ingwersen, J., Högy, P., Warrach-Sagi, K., Streck, T. and Wulfmeyer, V.: Three year observations of water vapor and energy fluxes over agricultural crops in two regional climates of Southwest Germany, Meteorologische Zeitschrift, 39–59, doi:10.1127/metz/2014/0618, 2015.

Wizemann, H.-D., Trebs, I. and Wulfmeyer, V.: Surface energy balance observations at a grassland site in Luxembourg, GFZ Data Services, doi:http://doi.org/10.5880/fidgeo.2018.024, 2018.

Wolf, A., Anderegg, W. R. L. and Pacala, S. W.: Optimal stomatal behavior with competition for water and risk of hydraulic impairment, PNAS, 113(46), E7222–E7230, doi:10.1073/pnas.1615144113, 2016.

Wulfmeyer, V., Turner, D. D., Baker, B., Banta, R., Behrendt, A., Bonin, T., Brewer, W. A., Buban, M., Choukulkar, A., Dumas, E., Hardesty, R. M., Heus, T., Ingwersen, J., Lange, D., Lee, T. R., Metzendorf, S., Muppa, S. K., Meyers, T., Newsom, R., Osman, M., Raasch, S., Santanello, J., Senff, C., Späth, F., Wagner, T. and Weckwerth, T.: A New Research Approach for Observing and

Deleted: Soc., doi:10.1175/BAMS-D-17-0001.1,

Deleted: :10.1016/j.agrformet.2012.11.004,

Deleted: :10.1080/01431161.2012.716529,

Deleted: :10.1002/qj.49709841510,

Deleted: :10.1016/j.rse.2006.11.028,

Deleted: :10.1127/metz/2014/0618,

Deleted: :10.1073/pnas.1615144113,

Characterizing Land–Atmosphere Feedback, Bull. Amer. Meteor. Soc., 99(8), 1639–1667, doi:10.1175/BAMS-D-17-0009.1, 2018.

Xiang, T., Vivoni, E. R., Gochis, D. J. and Mascaro, G.: On the diurnal cycle of surface energy fluxes in the North American monsoon region using the WRF-Hydro modeling system, Journal of Geophysical Research: Atmospheres, 122(17), 9024–9049, 2017.

Yang, Y., Long, D., Guan, H., Liang, W., Simmons, C. and Batelaan, O.: Comparison of three dual-source remote sensing evapotranspiration models during the MUSOEXE-12 campaign: Revisit of model physics, Water Resour. Res., 51(5), 3145–3165, doi:10.1002/2014WR015619, 2015.

Zhang, Q., Manzoni, S., Katul, G., Porporato, A. and Yang, D.: The hysteretic evapotranspiration-Vapor pressure deficit relation: ET-VPD hysteresis, Journal of Geophysical Research: Biogeosciences, 119(2), 125–140, doi:10.1002/2013JG002484, 2014.

Zheng, H., Wang, Q., Zhu, X., Li, Y. and Yu, G.: Hysteresis Responses of Evapotranspiration to Meteorological Factors at a Diel Timescale: Patterns and Causes, PLOS ONE, 9(6), e98857, doi:10.1371/journal.pone.0098857, 2014.

Zhou, C. and Wang, K.: Biological and Environmental Controls on Evaporative Fractions at AmeriFlux Sites, J. Appl. Meteor. Climatol., 55(1), 145–161, doi:10.1175/JAMC-D-15-0126.1, 2016a.

Zhou, C. and Wang, K.: Evaluation of Surface Fluxes in ERA-Interim Using Flux Tower Data, J. Climate, 29(4), 1573–1582, doi:10.1175/JCLI-D-15-0523.1, 2016b.

Zhou, C., Wang, K. and Ma, Q.: Evaluation of Eight Current Reanalyses in Simulating Land Surface Temperature from 1979 to 2003 in China, J. Climate, 30(18), 7379–7398, doi:10.1175/JCLI-D-16-0903.1, 2017.

Zhou, C., He, Y. and Wang, K.: On the suitability of current atmospheric reanalyses for regional warming studies over China, Atmospheric Chemistry and Physics, 18(11), 8113–8136, doi:https://doi.org/10.5194/acp-18-8113-2018, 2018.

Deleted: :10.1002/2014WR015619,

Deleted: :10.1002/2013JG002484,

Deleted: :10.1371/journal.pone.0098857,

Deleted: :10.1175/JAMC-D-15-0126.1,

Deleted: :10.1175/JCLI-D-15-0523.1,

Table 1: Variables provided by the surface energy balance station and used for this work.

Variable	Symbol	Unit
Horizontal wind components	u, V	m s^{-1}
Vertical wind	w	m s^{-1}
Sensible heat flux	H	W m^{-2}
Latent heat flux	λE	W m^{-2}
Ground heat flux	G	W m^{-2}
Upward shortwave radiation	R_{su}	W m^{-2}
Incoming shortwave radiation	R_{sd}	W m^{-2}
Upward longwave radiation	R_{lu}	W m^{-2}
Downward longwave radiation	R_{ld}	W m^{-2}
Friction velocity	$u*$	m s^{-1}
Air temperature	T_a	K, °C
Relative humidity	r_H	%
Surface air pressure	p	hPa
Precipitation	P	mm
Soil moisture (5, 15 and 30 cm)	θ	v/v
Soil temperature (5, 15 and 30 cm)	T_{soil}	K

Deleted: Surface shortwave albedo ... [1]

Table 2: Input variables used in the different evapotranspiration schemes.

Scheme	R_n	G	T_a	T_s	e_a	e_s	u	**Other parameters**
Priestley-Taylor	Obs	Obs	Obs					
Penman-Monteith (with constant g_s)	Obs	Obs	Obs		Obs	Obs	Obs	$g_{ah,Thom}$ = f(u,u*) (3), g_s = const
FAO Penman-Monteith	Obs	Obs	Obs		Obs	Obs	Obs	$g_{av} = u/208$, g_s = 1/70 m/s
OSEB	Obs	Obs	Obs	Obs			Obs	h_c
TSEB	Obs	Obs	Obs	Obs			Obs	f_c, f_g, h_c
STIC	Obs	Obs	Obs	Obs	Obs	Obs		

Table 3: Statistics for all days, and sunny wet or dry days based on 30min values during daytime hours 6:00-18:00. Performance statistics, root mean square error (rmse) and explained variance r^2 are computed with respect to the observed latent heat flux corrected for the closure gap by the Bowen Ratio (λE_{BRC}). As a reference we also provide statistics for the uncorrected, observed latent heat flux (λE_{uncor}). Potential evapotranspiration estimates are Priestley-Taylor (PT) and FAO Penman-Monteith (FAO-PM) reference evapotranspiration. Actual λE estimates are provided by the three schemes. Statistics are computed for all days and for clear-sky days classified as "wet" and "dry".

Statistic	**Period**	λE_{BRC}	λE_{uncor}	**PT**	**FAO-PM**	**OSEB**	**TSEB**	**STIC**
mean	all	178	145	259	224	202	204	170
mean	wet	264	213	325	294	255	259	218
mean	dry	164	134	315	285	212	209	180
rmse	all	0	40	106	81	41	43	46
rmse	wet	0	57	71	52	29	24	66
rmse	dry	0	33	169	140	57	58	45
r^2	all	1.00	0.94	0.72	0.62	0.85	0.84	0.72
r^2	wet	1.00	0.91	0.96	0.83	0.92	0.92	0.66
r^2	dry	1.00	0.93	0.75	0.56	0.62	0.61	0.44

Table 4: Results of the Camuffo-Bernardi regression model with mean (standard deviation) for wet and dry days. The slope of the variable against R_{sd} is represented by b (note that the unit of b depends on the unit of the variable) and the phase lag to incoming solar radiation is converted to minutes. The adjusted explained variance by the multi-linear regression model is given in column R^2. The phase lag to R_n-G is reported in the last column for comparison.

Variable	Moisture Conditions	Slope b	Phase Lag to R_{sd} (in min.)	R2adj	Phase Lag to R_n-G (in min.)
Net Radiation	wet	0.7162 (0.0106)	1 (3)	0.998	-2 (2)
	dry	0.6980 (0.0119)	-1 (2)	0.998	0 (1)
Soil Heat Flux	wet	0.1483 (0.0194)	-6 (8)	0.964	-8 (9)
	dry	0.1261 (0.0173)	-0 (8)	0.968	2 (7)
Available Energy	wet	0.5679 (0.0122)	3 (3)	0.998	-
	dry	0.5719 (0.0180)	-1 (2)	0.998	-
Sensible Heat Flux	wet	0.1715 (0.0275)	-22 (6)	0.964	-25 (7)
	dry	0.3388 (0.0470)	-3 (8)	0.988	-3 (8)
Incoming	wet	0.0340	133 (84)	0.600	124 (77)

Deleted: 225

Deleted: 295

Deleted: 286

Deleted: 82

Deleted: 141

Deleted: 55

Deleted: conditions

Deleted: Adjusted R^2

Inserted Cells

Longwave		(0.0092)			
	dry	0.0263 (0.0115)	176 (51)	0.459	158 (49)
λE BRC	wet	0.3992 (0.0186)	15 (4)	0.990	11 (3)
	dry	0.2380 (0.0317)	3 (12)	0.981	3 (11)
λE uncor	wet	0.3284 (0.0289)	14 (5)	0.967	10 (4)
	dry	0.1939 (0.0271)	2 (16)	0.963	3 (14)
Priestley-Taylor	wet	0.5354 (0.0279)	9 (5)	0.997	5 (2)
	dry	0.5238 (0.0414)	6 (4)	0.996	6 (3)
Penman-Monteith const. gs	wet	0.4326 (0.0371)	30 (9)	0.981	25 (6)
	dry	0.4288 (0.0456)	35 (11)	0.974	32 (10)
FAO Penman-Monteith	wet	0.4233 (0.0432)	31 (11)	0.980	26 (9)
	dry	0.4200 (0.0533)	31 (12)	0.981	29 (12)
λE OSEB	wet	0.3718 (0.0100)	9 (6)	0.976	5 (4)
	dry	0.2978 (0.0372)	-2 (5)	0.948	-1 (5)
λE TSEB	wet	0.3793 (0.0228)	9 (5)	0.989	5 (2)
	dry	0.2843 (0.0545)	1 (6)	0.962	1 (4)
λE STIC	wet	0.3037 (0.0695)	20 (19)	0.876	15 (19)
	dry	0.2387 (0.0655)	14 (14)	0.892	13 (12)
Air Temperature	wet	0.0088 (0.0008)	130 (41)	0.742	122 (41)
	dry	0.0084 (0.0017)	138 (35)	0.685	130 (37)
Surface Temperature	wet	0.0203 (0.0010)	51 (18)	0.923	46 (16)

Deleted: λE_{BRC}

Deleted: λE_{uncor}

Deleted: 5352

Deleted: 0278

Deleted: 5237

Deleted: 0412

Deleted: 3995

Deleted: 31 (8

Deleted: 982

Deleted: 0354

Deleted: 3888

Deleted: 0404

Deleted: 4241

Deleted: 0435

Deleted: 4211

Deleted: 0537

Deleted: Skin

	dry	0.0228 (0.0027)	51 (13)	0.933	49 (13)
T_s - T_a	wet	0.0116 (0.0013)	-22 (8)	0.966	-24 (10)
	dry	0.0145 (0.0017)	-10 (7)	0.973	-7 (7)
Vapor Pressure	wet	0.0003 (0.0015)	127 (186)	0.266	115 (183)
	dry	-0.0003 (0.0012)	52 (246)	0.316	71 (250)
Vapor Pressure Deficit	wet	0.0143 (0.0031)	145 (39)	0.791	134 (40)
	dry	0.0128 (0.0032)	153 (46)	0.719	144 (47)

Deleted: 125 (188

Deleted: 267

Deleted: 247

Deleted: 0371

Deleted: 53 (15

Deleted: 961

Deleted: 0059

Deleted: 0409

Deleted: 57 (19

Deleted: 953

Deleted: 0071

Page 35: [1] Deleted **AuthorRevision** **11/21/18 9:20:00 AM**